GENERAL REFERENCES

HIGH TEMPERATURE ALLOYS

1. Introduction

In general, the strength of most metals decreases with increasing temperature. At elevated temperatures, the increased rates of diffusion controlled and thermally activated processes result in the increased mobility of atoms and increased vacancy concentrations, and can activate additional slip systems or change slip systems (1,2). Furthermore, although grain boundaries can strengthen a metal at low temperatures, deformation at and along grain boundaries can occur more easily at high temperatures. Due to the more rapid diffusion rates at high temperature, particles or precipitates can coarsen, eventually resulting in an overaged condition with reduced strength. Lastly, at elevated test temperatures, significant interactions between the metal and the environment can occur. Rapid oxidation

of the surface or grain boundary penetration can occur at elevated temperatures and will result in reduced strengths and perhaps reduced ductilities.

When considering the high temperature strength of a material, it is also necessary to consider some sort of time scale. At room temperature, the deformation of most materials is independent of time or the rate of deformation (ie, strain rate), for most practical purposes. The tensile properties of a material will remain relatively unchanged even if strain rates are changed by orders of magnitude. However, at elevated temperature, the strength of a material is strongly dependent on strain rate, time of exposure and the test temperature. In some respects, metals at elevated temperature exhibit a viscoelastic type of behavior, similar to polymeric materials at low temperature. Materials that are exposed to stresses at elevated temperatures exhibit creep, which is an undesirable time-dependent plastic deformation (3). Generally, creep pertains to deformation at strain rates less than 0.01/minute. As an example, the turbine blades on the spinning rotor of an operating gas turbine, which may be at temperatures up to 1200°C, slowly grow in length due to creep. The blades must eventually be replaced before they make contact with the turbine case (housing). Typical elevated temperature structural applications include power generation plants, aircraft and rocket propulsion, airframes and automotive engines.

Although creep can occur at almost any temperature, the full effects of creep deformation is observed at homologous temperatures in excess of about 0.4 ($= T/T_m$). The homologous temperature is the ratio of the test temperature, T, and the melting point (T_m) of the pure element or the solidus of an alloy.

The materials selected for high temperature applications, are typically referred to as high temperature alloys, are known for their ability to resist, and exhibit useful strengths at, elevated temperatures. In general, the physical properties of the elements that could be utilized as the alloy base for high temperature materials include melting temperatures, elastic modulus, and density. Some of these properties are more important than others, depending on the application. For example, if the alloy is being considered for a rotating component or for an airframe for an aerospace application, the density becomes very important since the stresses from centrifugal forces or payload capabilities. In addition, although a high melting temperature would be expected to be essentially a requirement, an element with a high melting point, does not necessarily make the element a candidate for elevated temperature service, particularly when considering an application in air. The primary reasons for this discrepancy are that many times an element may exhibit an allotropic phase transformation below its melting point, nonprotective surface oxide growth, a nonclose packed crystal structure and/or only limited solubility for elements that could strength it by the formation of a solid solution or form strengthening precipitates. The modulus of the alloy is important for several aspects of design, including determining the amount of deflection that occurs during elastic loading and calculation of thermally induced stresses. Lastly, the modulus may also provide an indication of the temperature capabilities of the alloy since the modulus is related to the bond strength of the atoms.

Additional considerations for the selection of a high temperature alloy system include thermal conductivity and thermal expansion coefficient. In most cases, it is desirable for an elevated temperature material to exhibit a high thermal conductivity and a relatively low coefficient of thermal expansion. Within a

component operating at high temperature, thermal gradients can develop during steady-state operation and during changes in operating conditions. In either case, the thermal gradient can result in significant thermal strains and thermal fatigue. Increased levels of thermal conductivity can lessen these thermal gradients, resulting in reduced thermal strains. In addition, as a component is heated to the operating temperature, it will expand. The fit-up of components and the gaps that are designed in to elevated temperature systems must incorporate the coefficient of thermal expansion for all of the components in the system. Utilizing alloys with reduced coefficients of thermal expansion may simplify the design.

Although it does not display a particularly high melting point, Ni has been, and will continue to be, the preferred alloy base for high temperature alloys. The primary reason for the selection of Ni, as the preferred alloying system, is the lack of an allotropic phase transformation below its melting point, its high tolerance for a wide variety of alloying elements without causing any phase instability, the close-packed face-centered cubic (FCC) crystal structure and the ability to produce and manipulate a very stable precipitate γ'-Ni_3(Al,Ti,-Ta,Nb), which is one of the primary sources of elevated temperature strength in Ni-base superalloys.

2. Creep

In general, metals and alloys exhibit a significant reduction in strength at elevated temperatures and it is also necessary to consider some sort of time scale. At elevated temperature, the strength of a material is strongly dependent on strain rate, time of exposure, and the test temperature. In some respects, metals at elevated temperature exhibit a viscoelastic type of behavior, similar to polymeric materials at low temperature. Materials that are exposed to stresses at elevated temperatures exhibit creep, which is an undesirable time-dependent plastic deformation (3). Generally, creep pertains to deformation at very low strain rates (eg, less than 0.01/min).

Although creep can occur at almost any temperature, the full effects of creep deformation is observed at homologous temperatures in excess of about 0.4 ($= T/T_m$). The homologous temperature is the ratio of the test temperature, T, and the melting point (T_m) of the pure element or the solidus of an alloy. The creep behavior of a material is generally defined as the time to failure and the fracture strain as measured during experiments. In some cases, the time to given amounts of strain and strain rates are also measured.

In general, an increase in the temperature results in increased creep deformation rates, since the material strength generally decreases with increasing temperature. In addition, increased stresses will result in increased creep deformation rates. Hence the time to rupture will decrease with increasing test temperature and/or stress. For design purposes, it is necessary to perform numerous creep tests at several stresses, at several temperatures. Frequently, materials selection for an elevated temperature application is based on the creep properties rather than the tensile properties. Often times, it is helpful for design to represent the creep data as a time–temperature parameters (TTP) which allow for extrapolation and interpolation of shorter time creep data (4-10). Many applications require component lifetimes of 10,000+ hours, however, the cost and time

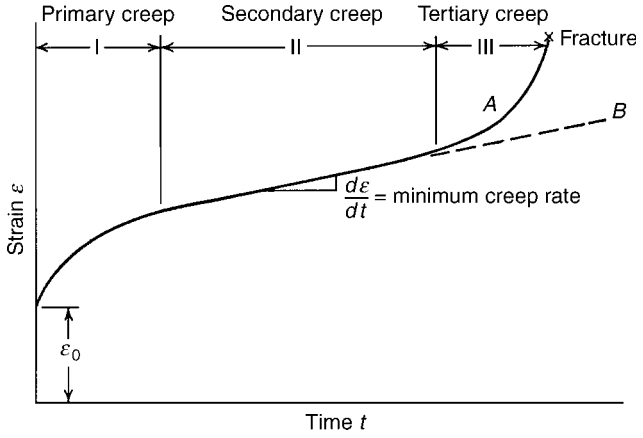

Fig. 1. Schematic drawing of typical creep curves for constant-load creep (Curve A) and constant-stress creep (Curve B) (13). Note the three regions of the creep curves and the creep rate.

required to develop a database with numerous 10,000+ hour tests is prohibitive. Therefore, there is a need to extrapolate shorter term creep test data to component lifetimes.

2.1. Analysis of the Creep Curve. Idealized creep curves for both constant stress and constant load tests are shown in Figure 1 (11,12) . The constant load curve is indicated as curve A and curve B is for constant stress. The slope of the curves ($\partial\epsilon/\partial t$) is referred to as the creep rate and is the instantaneous rate at which the sample is deforming in creep. Following an initial rapid elongation of the sample, ϵ_0, the creep rate decreases with time, then reaches essentially a steady state in which the creep rate changes little with time. In some cases, the creep rate does not remain essentially constant, but slowly increases with time (and deformation). Finally, the creep rate increases again rapidly with time until fracture occurs. Frequently, the failure of a creep sample is referred to as a rupture. Based on these different types of creep behavior, the creep curve is usually broken down into three sections. The first stage is referred to as primary creep and includes the initial deformation and the decreasing creep rate. The second stage is typically when the minimum and/or the steady state creep rate is observed. The final stage or tertiary creep state include the increasing strain rate, leading to failure. The difference between constant stress and constant load is observed in the tertiary creep region (Fig. 1). This difference occurs due to the decreasing gage section diameter during the plastic deformation. The constant load sample exhibits the increasing creep rate during tertiary creep since the stresses are continuously increasing. Although the load is maintained constant, the cross-sectional area of the gage section is continuously decreasing resulting in an increasing stress. However, in the constant stress test, the constant stress is maintained by reducing the load as the sample deforms and the cross-sectional area decreases during the test. It should be noted that creep tests can be performed in either a tensile stress or a compressive stress. During a compressive creep test, though, the sample diameter increases as the sample deforms, which decreases the stress for constant load samples.

2.2. Definition of Stress and Strain. Similar to the tensile test discussions, the stress has units of force per unit area. However, only engineering stress is used as an appropriate measure in creep testing. The engineering stress is the load divided by the original gage section area. The engineering strain is measured as the increase in gage section length divided by the original length. The engineering strain can also be determined from the change in gage section area divided by the original gage section area. In addition, at the start of creep tests, the modulus can be estimated from the loading curve as the load is applied. Since the sample is heated to the test temperature at relatively low load to prevent deformation during the heat-up, the sample must be loaded prior to starting the test. The deflection is measured as a function of the load as it is applied and the results can then be used to determine the modulus. Once the loading is complete, the test is started and the clock begins to record the duration of the test. Throughout the creep test, the deformation strain and the strain rate are recorded as a function of time. When the sample fails, or ruptures, the clock is stopped and the rupture time is recorded. In addition, the last strain measurement or rupture strain (ductility) is recorded. The failed sample is then measured to determine the elongation and the reduction in area. Lastly, the measured rupture strain is compared to the recorded rupture strain.

2.3. Factors Effecting the Curve. The strain versus time curve that is obtained during a creep test depends on the material and its microstructure and the temperature and initial stress of the test.

In some cases, the first two variables are considered intrinsic to the test. Modification to the either of these two variables will have a significant change to the creep test results without changing the type of test or test machine. However, changing the characteristics of the test machine will result in creep data that are similar for most of the test. Significant differences between different types of creep machines are frequently only seen in the tertiary stages of creep.

2.4. Materials and Microstructures. The material and the microstructure have a profound effect on the shape of the strain versus time curve and the creep strength. A schematic representation of the creep strength of a variety of materials is shown in Fig. 2. In general, the creep resistance of a material scales with the melting point and modulus. Increased creep resistance is seen in materials that exhibit an increased modulus and high melting temperatures. In addition, more densely packed crystal structures exhibit increased creep resistance (eg, body-centered cubic versus face-centered cubic). Unlike tensile strength, finer grain sizes do not result in increased creep resistance since the strength of the grain boundary decreases with increasing temperature. Although the grain boundaries strengthen metals at low temperatures, the grain boundaries weaken the material at high temperature. Coarse grain sizes typically exhibit increased creep resistance. At the extreme, the highest creep strengths are observed in sample with either grain boundaries parallel to the stress direction (ie, columnar grained materials) or samples without grain boundaries (ie, single crystals). Cold work is also not an effective way to increase the creep strength of a material. At elevated temperatures, any residual cold work will likely result in recovery, recrystallization and grain growth. Some of the strengthening mechanisms that do result in increased creep resistance are solid solution hardening, precipitation hardening, dispersion hardening, and order hardening. Solid

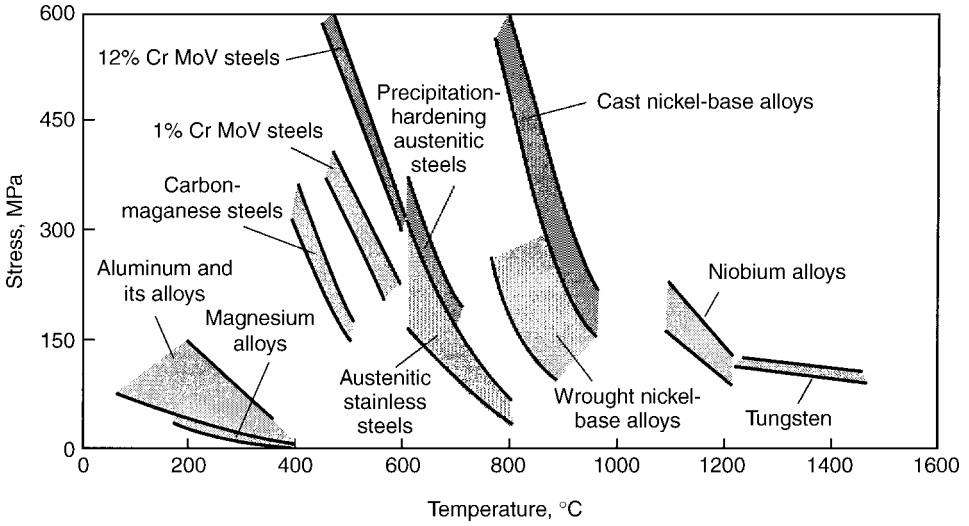

Fig. 2. General trends in the creep strength for several classes of structural materials. The stress reported are the stresses required to produce rupture in 1000 hours (1).

solution strengthening results in increased creep strength due to local changes to the modulus and lattice parameter, and modification of the stacking fault energy and melting temperatures. As noted previously, precipitation hardening results in increased tensile properties, but also results in increased creep resistance in most cases. At high temperatures, excessive misfit between the precipitate and the matrix will result in changes in the precipitate morphology over time. Eventually, the precipitates will lose their ability to strengthen the matrix. Precipitates that are stable can result in increased creep resistance due to the difficulty in deforming the precipitates. A dispersion of hard particles, such as oxides, carbides, nitrides or borides can also result in increased creep resistance. In addition, the presence of order in the atomic arrangement in the lattice will also result in increased creep resistance to slowed diffusion rates, and in some cases, an increased modulus. In general, any method that strengthens a material in tensile testing, will result in increased creep resistance, if the strengthening mechanism is stable at high temperatures.

2.5. Effects of Temperature and Stress. An increase in either the stress or the temperature will result in more rapid creep deformation and shorter times to rupture (Fig. 3). Since creep deformation is dependent on thermally activated process, increased temperatures increase the rates of creep deformation. It should be noted that all three of the stages will not be found in all cases. The presence of each of the three stages of creep deformation is strongly dependent on the stress and temperature. In general, the lower stresses, and/or lower temperatures, exhibit better defined stages and longer steady state creep regimes than the higher stress/temperature tests.

2.6. Practical Aspects of Determining the Creep Behavior of a Material. There are three basic types of common creep tests. The creep test and the rupture test are very similar and can be run on the same test machines.

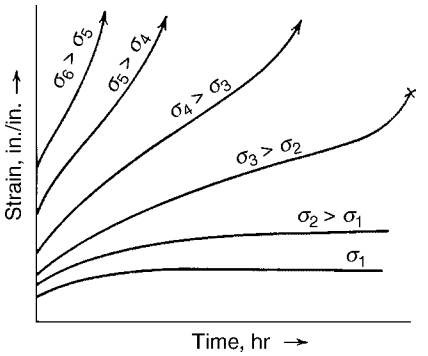

Fig. 3. Schematic strain versus time creep curves indicating the effect of increasing stress on the creep behavior of a material at constant temperature (13). Note that increasing the stress not only shortens the creep life, but also may eliminate some of the three regions typically seen in a strain versus time creep curve.

The stress relaxation test will produce data very similar to the creep test, but requires extensive modification to the creep test frame.

The Basic Creep Test. A creep test consists of loading a specimen at a specified load and temperature and measuring the displacement as a function of time and the time to failure, sometimes called rupture. This type of testing is well documented in the ASTM E139 standards (13). The load frame can either impose a direct load on the sample or can use a lever arm to multiple the load being applied to the specimen. The test can be run with a constant load, usually applied by a dead weight load or by mechanical means. Creep tests can also be performed under constant stress conditions, but the applied load must be continuously adjusted during the test. The load must be decreased so that the stress remains constant as the sample area decreases due to the plastic deformation when the test is being performed in a tensile mode. It is also possible to perform the test with compressive stresses with modified fixturing. Compression creep testing is frequently done when testing brittle materials or when only very limited amounts of test material are available. Unlike tensile creep testing, the cross-sectional area of the sample increases with deformation. Therefore, during constant stress, a creep test requires the load to increase with the increasing cross-sectional area of the sample. In general, though, most creep testing is performed in tension.

The progressive deformation of the sample at constant load (or stress) is called the creep strain. The primary output from the creep test is a record of strain versus time, as shown in Figure 1. The strain is measured by attaching an extensometer using a mechanical frame connecting the sample to an LVDT, dial gage or some other technique of measuring strain. The output from the LVDT can be fed into either a chart recorder or a data acquisition system for subsequent analysis. A test operator will have to manually record the strain readings from a dial gage. However, readings must be taken frequently to ensure that a reasonable creep curve is produced.

After the sample has failed, the dimensions of the fractured sample are carefully measured and compared to the measurements of the sample prior to testing. The elongation and reduction in area of the gage section can then be determined. The measured ductility is then compared to the data recorded from the LVDT.

In general, test durations can vary between approximately 10 hours up to 100,000 hours or more for creep tests. However, most creep tests last between 10 hours and 10,000 hours. The cost to perform 10,000+ hour tests is generally very prohibitive and tests of this duration are rarely performed.

The Basic Stress Rupture Test. The stress rupture test is very similar to the creep test, except that the creep strain is not measured during the test. The stress rupture test also consists of loading a specimen at a specified load and temperature, but only the time to failure is measured. The rupture ductility is measured by comparing the separation of gage marks, sample length, or some other feature before and after testing. Similar to creep testing, test durations can vary between approximately 10 hours up to 100,000 hours or more. However, most tests last between 10 hours and 10,000 hours.

In some cases, the effect of notches or stress concentrations on the rupture properties of the material is also evaluated. Two types of samples can be used for the evaluation of stress concentrations. A sample with a single notch can be tested. The time to rupture of the notched sample is then compared to that of the sample without the notch. If the material exhibits a reduction in the creep life, the sample is considered notch sensitive. If on the other hand, the notched sample exhibits an creep test lifetime greater than that of the un-notched sample, the material is considered notch strengthened. The material is considered uneffected by a stress concentrator if the presence of the notch does not have any significant effect on sample lifetime. Note that this technique, requires the testing of two samples. An alternative technique which requires a reduced number of test samples is to utilize a sample design with two gage sections, one with a notch and one without a notch or a smooth gage section. Extreme caution must be used when machining the combination sample. The cross-sectional area of the notch must be the same as the un-notched gage area, in order to prevent biasing of the test results. If the sample is notch sensitive, failure will consistently occur at the notch. Notch strengthening occurs with the sample consistently fails in the smooth gage section. Otherwise, the sample will fail in a random manner at both the smooth, un-notched gage section and the notched gage section when the materials is not influenced by the presence of a stress concentrator.

The cost of performing a stress rupture test is significantly less than the creep test, since the time to set-up and the equipment utilized during the test is reduced. However, the amount of data produced by the stress rupture test is also significantly less than the creep test. In most cases, stress rupture testing is used for screening large numbers of samples, materials and/or test conditions. Creep testing is most commonly done for scientific reasons to understand deformation mechanisms and for design purposes.

The Basic Stress Relaxation Test. Creep testing to determine the effects of stress and temperature on the creep rate, time to specified creep strains and time to rupture of a given material in a given condition can be very time consuming and very expensive. Numerous samples must be tested under a variety of test

conditions, which will require many creep frames. Stress relaxation testing offers the potential to reduce the number of tests and the time to complete the testing by using a single sample to determine a wide range of strain rate versus stress data. Unlike creep testing, where a fixed load (or stress) is applied and the strain monitored, stress relaxation testing applies a fixed strain and the load is monitored. The initial elastic loading of the sample to a fixed length is converted to plastic strain, which results in a reduction of the load. The initial displacement is usually based on the deformation corresponding to a given load (or stress). The load is then monitored as a function of time, which is used to determine the stress versus strain-rate data. A significant amount of data can be accumulated from only a few samples in a very short time. However, creep testing data and the stress relaxation data are frequently not in agreement. Very precise temperature control and load measuring techniques are required. In addition, the loading rate of the sample has a significant effect on the properties and may result in significant errors. Lastly, the stress relaxation testing can determine very low creep rates in a very short period of time. Similar data from creep testing, would require significant numbers of samples and long-term testing. However, the short duration of the stress relaxation test may not be a representative test condition for long-term elevated temperature service. The long-term creep tests may be a more accurate method to evaluate the service condition, since microstructural evolution can occur and any microstructural instabilities may not be observed in the much shorter-term stress relaxation test. In general, a combination of both creep testing and stress relaxation testing would be a more productive way of generating a large amount of data on the creep properties of a material.

Environment. Creep and stress rupture testing is also carried out in various environments, including vacuum. Since environmental attack of the test material can occur at elevated temperatures, the environment selected for testing can be either to simulate the actual use conditions, evaluate the effects of the environment on the properties or to eliminate any environmental effects and evaluate only the material behavior. An environmental chamber is utilized which can either enclose just the sample, grips and fixturing or enclose the furnace, as well as, the sample, grips and fixturing. When the environmental chamber is inside the furnace and encloses only the sample, grips and fixturing, it is considered a hot wall design, since the chamber is heated to the same temperature as the sample. In such cases, selection of the chamber material is critical since it will also interact with the air environment on the outside of the chamber and the selected environment on the interior. Ceramics (eg, Al_2O_3) and Ni-base superalloys are frequently utilized for the chamber. Cold wall chambers enclosed the furnace, as well as the sample, grips and fixtures. The cold wall designs frequently utilize water cooled walls which maintain the desired environment. Cold wall chambers are typically more expensive than hot wall designs, but do not interact with the test environment.

2.7. Creep Data Analysis. The use of creep-rupture properties to determine the allowable stresses for service parts has evolved with experience; however, the guidelines for each use differ among the specifications. For example, elevated temperature applications for pressure boundaries must utilize the ASME Boiler and Pressure Vessel Code (14), which limits the maximum stress

to the minimum of the following: (*1*) 100% of the stress to produce a creep rate of 0.01%/1000 hours. (*2*) 67% of the average stress or 80% of the minimum stress required to produce failure at 100,000 hours, as determined by extrapolated data.

There is a substantial database of the properties of high temperature alloys with data obtained from tests ranging from a few hours up to a few thousand hours (4-10). Creep tests are rarely run longer than 10,000 hours and test durations of 100,000 hours are very uncommon due to the expense and time required to perform the tests. Allowable stresses recommended in most existing specifications are derived from extrapolations. Considerable scatter in test results can be observed, even for a given heat of an alloy, so interpolated creep and rupture strengths are not precisely known. Due to the data scatter, extrapolation of creep data to longer times is even more difficult (4,5).

The scatter that can be observed in creep and rupture properties is generally due to a variety of reasons, including heterogeneities, sample size, test temperatures and heat-to-heat variations (15). The measured creep lifetimes for two samples tested under identical conditions may vary by about 15–25%; however, much larger variations can be observed. In most cases, it is not economically possible to test materials in the exact condition and for test times approaching the actual desired component lifetime, which may be in excess of 100,000 hours. Accurate means to extrapolate the creep data to the target component lifetime are necessary. No single method for determination and prediction of properties exists. However, a variety of techniques have evolved for manipulation of test data for most materials and structural applications of engineering significance. The most commonly used techniques are time-temperature parameters (TTPs).

The creep data that will be extrapolated are typically obtained on an accelerated time basis, by using higher test temperatures and stresses during constant load, isothermal, uniaxial creep tests. Combining the test temperatures and times into a parameter or an expression, can produce a single master curve of the creep properties for a given material. These master curves can then be used to compare the properties of several different materials or different heats of materials.

The development and use of the time–temperature parameters have been summarized in several review papers (16,17). Conceptually, though, the time–temperature parameters have a physical basis in chemical rate theory. Most of the parameters are loosely based on the Arrhenius equation, with several suitable, but nonrigorous, assumptions. To date, numerous TTPs have been developed and proposed. However, the most commonly used TTP's are based on the following five linear parameters:

(*1*) Larson-Miller Parameter ($P_{LM} = f(\sigma) = T_{Abs}(\log t + C)$)
(*2*) Manson-Haferd Parameter ($P_{MH} = f(\sigma) = (\log t - \log t_1)/(T - T_1)$)
(*3*) Orr-Sherby-Dorn Parameter ($OSD = f(\sigma) = t\exp(-Q/RT_A)$)
(*4*) Manson-Succop Parameter ($f(\sigma) = \log t - BT$)
(*5*) Goldhoff-Sherby Parameter ($f(\sigma) = (\log t - \log t_1)/(1/T - 1/T_1)$)

Where, σ is the applied stress, t is time, T is temperature in °C or °F, T_A is temperature in K or °R, Q is the activation energy, R is the gas constant and T_1,

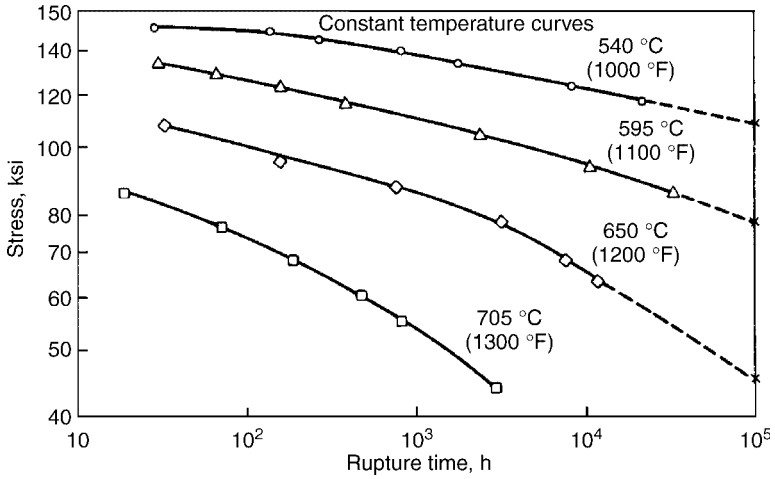

Fig. 4. Typical stress versus rupture time for the Ni-base superalloy, IN 718 (1). Note that several tests are performed at each test temperature, and that increasing the test temperature or increasing the stress results in reduced creep life.

t_1, B and C are numerical constants characteristic of the material and its condition. The numerical constants are determined by curve-fitting, graphical optimization or convergence, which can result in significant errors.

The Larson-Miller parameter, which is probably the most widely used TTP, was introduced in 1953 to correlate and extrapolate creep rupture data (10). To develop a Larson-Miller parameter for a material, an extensive creep test database must exist (Figs. 4 and 5). Constant stress lines on a graph of log t versus $1/T_A$ should converge to a point at $1/T_A = 0$. At this point, $\log t = C$ defines the optimum value of the constant, C, for the data being considered. Note the value of the constant, C, should be independent of stress. Typically, the value of the constant, C, range from 15 to 30. Frequently, a value of 20 is assumed for the constant when insufficient data exists to determine C. However, it is often not possible to determine a single value of the constant, C (4,5,10), which makes the extrapolation of data difficult.

Although the TTPs can be used to correlate time, temperature and stress in creep testing, extreme care must be taken. One additional concern that is not addressed by any of the TTPs, is metallurgical stability. Curvature in the isothermal stress-rupture lines may be observed when topologically close packed (TCP) phases form, beyond the point at which creep data are available. Since the parameters can not represent effects that are not observed during the short term testing used to develop the constants, it does not guarantee the reliability of extrapolation beyond that range. In addition, these parameters do not address the metallurgical effects of defects, such as pores, inclusions, etc, on the properties of the samples.

Another method used to represent creep data is the deformation map, which is a plot normalized stress (divided by the modulus) versus normalized or homologous temperature (divided by the melting point or solidus). Constant

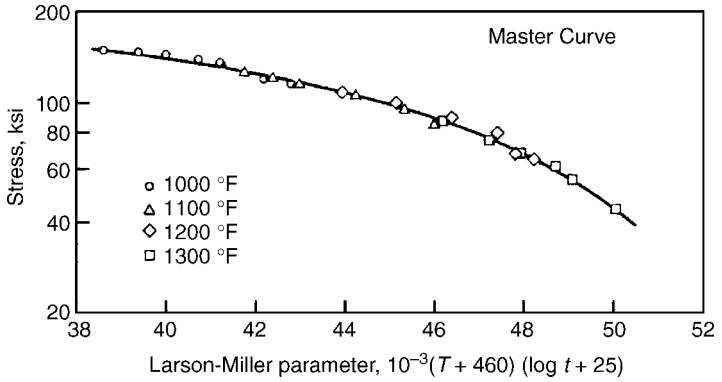

Fig. 5. Resulting Larson-Miller plot of IN 718 stress rupture data from Figure 5 (1). Note that all of the creep test data can be plotted onto a single master curve which can be used for extrapolation and interpolation of the creep data.

strain rates are plotted as contours on the deformation map which identify the deformation mechanism controlling the creep deformation. The deformation maps, typically show two main creep areas which differ in the deformation mechanism. The effects of the strengthening mechanisms, such as solid solution strengthening or precipitation hardening, can be seen by the shifting of the boundaries of these creep deformation areas. However, a very extensive database is required to produce the deformation maps. At this time, a limited number of materials can be accurately represented with deformation maps.

Probably the biggest source of errors when determining the creep properties of a material is the method of data representation and the use of time–temperature parameters. As noted above and in the identified references, the representation of the creep data and the use of time–temperature parameters can result in very inaccurate representations. The data generated may be extremely accurate, but the method of data representation and data manipulation can result in significant errors. The use of time–temperature parameters requires a significant database for the determination of the constants and the selection of the appropriate parameter. Comparison of data from various alloys, when utilizing a constant that is considered the "universal" constant, such as $C = 20$ in Larson-Miller parameters, can result in alloy selection or design stresses that are inappropriate. Extreme care must be taken when comparing, extrapolating and/or interpolating creep data that are generated under differing conditions and temperatures.

3. Fatigue

Structural materials are rarely subjected to constant or steady-state monotonic loads. In most cases, the magnitude, direction and number of loading axes vary with time. Most materials subjected to repetitive, alternating, vibrational or fluctuating stresses and temperatures will fail at stresses much lower than that

required to cause failure in a single application of load, such as a tensile test. These dynamic loads are considered fatigue loads, since they result in fatigue failures that occur after a considerable period of time. The occurrence of fatigue failures have been more and more common as the number and complexity of engineering systems, such as aircraft, vehicles, pumps, etc, have increased. It has been stated that approximately 90% of service failures due to mechanical causes can be attributed to fatigue (18).

Frequently, fatigue failures are particularly difficult to predict and can occur without any warning or indication and at stress levels that are often quite low. Analysis of the fracture surface can also be quite confusing, since the fracture often appears to be brittle, with little no gross plasticity. The fatigue failure can sometimes be recognized by a flat fracture surface with several distinct regions. The flat fracture surface can have regions that are essentially smooth, even at high magnification, due to the rubbing action of the fracture surfaces as the crack propagates. In some cases, a series of rings or beach marks are observed on the fracture surfaces which indicate the progress of the crack as the material was cycled in service or test. The beach marks are often times can be followed back to the initiation site, which usually is a point of stress concentration. Typical fatigue crack initiation sites include both microstructural stress concentrators, such as inclusions, coarse carbides, grain boundary triple points and porosity, and macroscopic stress concentrators such as machining marks, sharp corners and notches.

In order for fatigue to occur the stress imposed on the material must have tensile and cyclic components that are sufficiently large to cause fatigue damage. In addition, it is necessary to accumulate enough cycles to initiate and propagate a fatigue crack. Other factors than can affect the fatigue behavior of a material include temperature, environmental interactions, stress concentrators, microstructure, overload, residual stresses and combined stresses. It is not possible to perform tests in a laboratory that can completely replicate the service environment. Therefore, often times, several of these factors are not included and only a few test variables are evaluated at a time.

3.1. Principles of Fatigue Testing. Fatigue can be broken down into three regions; fatigue crack initiation, fatigue crack growth, and overload. The fatigue behavior can be represented as a range of the applied stress or strain versus the number of cycles to failure or the rate of fatigue crack growth versus the applied stress intensity at the crack tip. The fatigue behavior when plotted as a stress (or strain) range versus number of cycles (or reversals) to failure is commonly called an "S-N" curve (Fig. 6). For design purposes, it is necessary to understand how various service environments, loading spectrum, component design, alloy content and metallurgical details effect the fatigue properties of candidate alloys. To select an alloy, it would be helpful to be able to rank several alloys in terms of fatigue properties, in addition to other mechanical properties (eg, tensile, creep, toughness, etc). In order to evaluate alloys and begin to rank them, the testing must be performed in a laboratory environment that yields reproducible results. The testing will likely require a simplification of the loading and/or service environment.

Cyclic Stresses and Strains. Similar to the tensile and creep test discussions, the stress has units of force per unit area and is primarily based on the

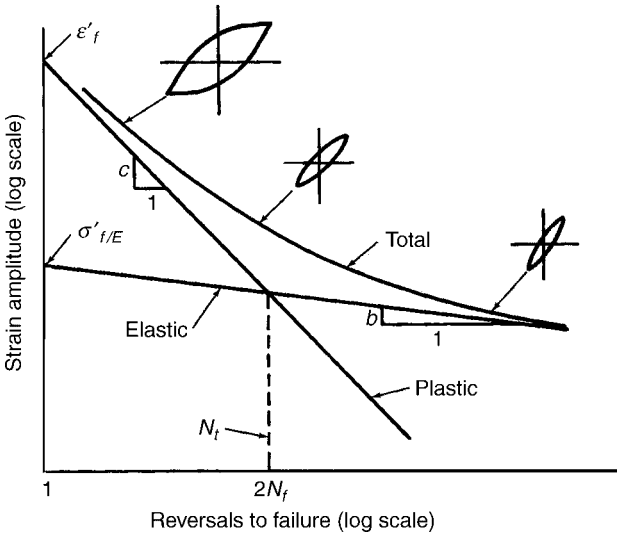

Fig. 6. Schematic representation of a fatigue strain life (ϵ-N) curve. Note that the curve is a summation of the elastic and plastic portion of the fatigue behavior. Also, note that the curves refers to reversals, which is equivalent to double the number of cycles.

engineering stress. The engineering stress is the load divided by the original cross-sectional area and can be a tensile stress or a compressive stress. In addition, the stress can be normal stress in which the stress is acting perpendicular to the plane of interest or the stress can be in the plane, which is a shear stress.

The strain measured in fatigue testing is also almost exclusively engineering strain and utilizes the original cross-sectional area and/or the original gage length. Similar to the stresses, both compressive and tensile strains are utilized in fatigue testing. The engineering strains are calculated as the change in gage length divided by the original gage length or the change in the cross-sectional area divided by the original cross-sectional area. Most commonly the strains are normal strains, but on some occasions, shear strains are utilized.

Since fatigue testing involves applying a cyclic load or strain, it is necessary to characterize the loading cycles. As noted previously, it is not possible to recreate the service environment and loading. Therefore, simplified loading cycles, which can be recreated in a laboratory are used. A schematic representation of a fatigue load cycle is shown in Figure 7. The cycles are usually sinusoidal or saw-tooth and may include holds at the maximum load or strain. In order to fully characterize the cycle, several terms must be defined and controlled. The cyclic range, or $\Delta\sigma$, is defined as the difference between the maximum stress, σ_{max}, and the minimum stress, σ_{min}. The mean stress, σ_{mean}, is defined as $(\sigma_{max}+\sigma_{min})/2$ and the amplitude is $\Delta\sigma/2$. The ratio of the minimum stress to the maximum stress is the R-ratio $(=\sigma_{min}/\sigma_{max})$ which indicates if the stresses are all tensile or if the stresses are both compressive and tensile. When $R = 0$, the minimum stress is zero. A fully reversed cycle occurs when $\sigma_{max} = -\sigma_{min}$ and $R = -1$. Note that similar characterizations of the loading waveform can

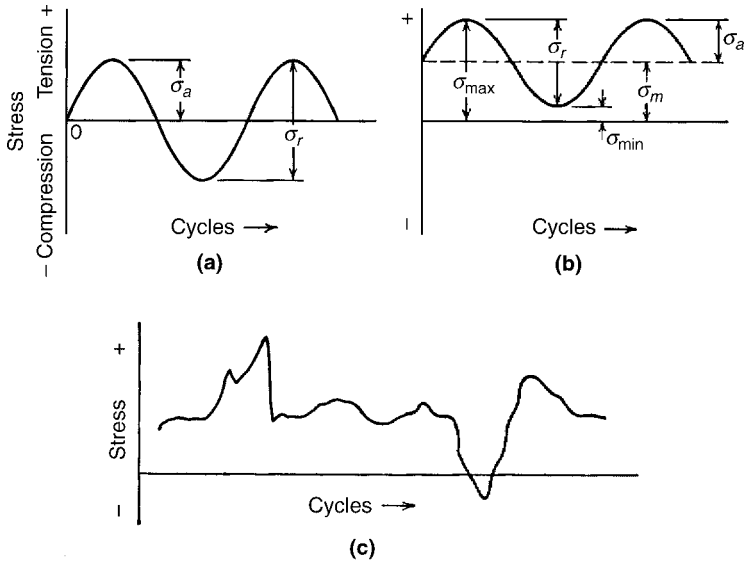

Fig. 7. Schematic representation of typical fatigue stress (loading) waveforms. The fully reversed (R-ratio=−1.0) is shown in (**a**), which is typically used for LCF testing. The waveform used for HCF and FCGR testing is shown in (**b**) in which the R-ratio and the mean stress is greater than zero. A random fatigue cycle is shown in (**c**).

be made when using strain control, by using the ϵ_{min} and ϵ_{max} in place of the σ_{max} and σ_{min}. For example, the R-ratio is equal to $\epsilon_{min}/\epsilon_{max}$ and the strain amplitude ($\Delta\epsilon/2$) is the one-half of the difference between ϵ_{min} and ϵ_{max}.

When determining the fatigue crack growth rate during a test, the rate of crack advance per cycle (da/dn) is correlated with the stress intensity at the crack tip (Fig. 8). Most fatigue crack growth tests are performed in load control, where specified maximum and minimum loads are applied to the sample using the appropriate waveform. The crack has a length, a, and the number of cycles, n, are counted to make the crack grow a given distance, Δa, which is then used to determine the rate of crack growth (da/dn). The stress intensity at the crack tip is calculated from the length of the crack, load applied, the geometry of the test sample and the mechanical properties of the materials. Similar to the stress range, the stress intensity range, ΔK, is reported as a function of the load range, crack length, sample geometry and mechanical properties of the material.

Factors Effecting Fatigue Behavior. The fatigue behavior of a material is effected by the following variables: (*1*) The test materials and its microstructure. (*2*) The test temperature (Note that at elevated temperature there can also be an interaction of the temperature, loading wave-pattern and the environment.) (*3*) Sample size and surface finish. (*4*) The stress or strain range and of the test.

Each of these variables are briefly discussed below in more detail. It should also be noted that fatigue test results are typically statistical in nature and significant variability in test results can be observed. Since the fatigue life and fatigue data, in general, are statistical quantities, it is necessary to determine the fatigue properties of a material with numerous samples. Fatigue properties

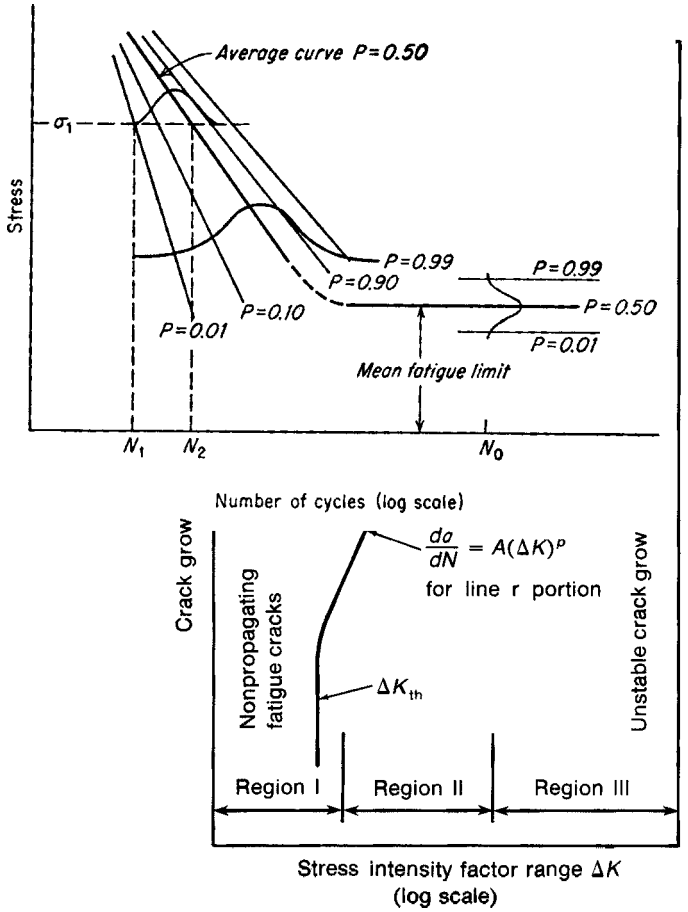

Fig. 8. Schematic representation of fatigue crack growth behavior of a material tested in a non-aggressive environment. Note that the crack growth rate increases as the stress intensity factor increases. A threshold regions (Region I), occurs when the crack is growing very slowly and is relatively short in length. As the crack continues to grow the stress intensity increases and the crack growth rates increase (Region II). In Region II, the crack growth rate becomes linear in the Paris Regime. Finally, the crack grows until the crack growth becomes unstable and crack growth rate increases and fracture occurs (Region III).

determined from just a few samples will result in considerable uncertainty. It is, therefore, more appropriate to consider the probability of a sample attaining a certain fatigue life (N_f or number of cycles to failure) at a certain stress/strain range. Fig. 9 illustrates the statistical nature of fatigue for a ferrous-based alloy that exhibits an endurance or fatigue limit. The probability of failure (P) ranging from 1% (P = 0.01), to 99% (P = 0.99), including the average (P = 0.50) are shown.

Materials and Microstructures. Fatigue properties are very sensitive to both the material and the microstructure. As noted above, ferrous-based alloys can exhibit an endurance limit in fatigue testing that is not exhibited in non-ferrous-based alloys (Fig. 10). In some cases, metallurgical changes (eg, refinement

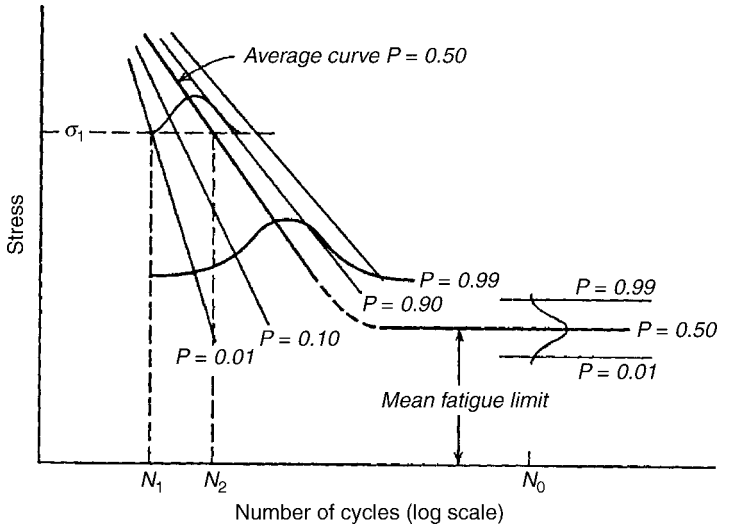

Fig. 9. Schematic representation of probability basis of fatigue data. Note that there is a potential for significant variation in the fatigue properties of all materials.

of the grain size) can result in significant improvements in fatigue properties. However, some metallurgical changes can improve some aspects of fatigue properties, but degrade others. Therefore, metallurgical changes must be made with care and with sufficient data to validate the changes.

In many cases, the fatigue properties of a material are correlated with its tensile properties. For cast and wrought ferrous alloys, the endurance or fatigue limit is usually assumed to be approximately 50% of the ultimate tensile

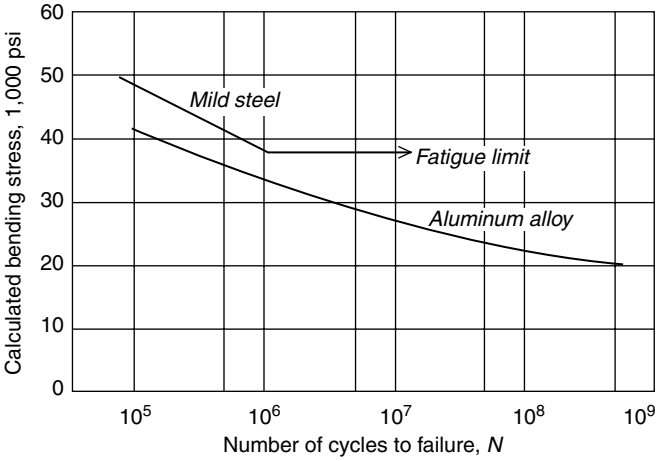

Fig. 10. Typical fatigue behavior of ferrous (mild steel) and non-ferrous (Aluminum alloy) metals. Note that the mild steel exhibits a fatigue limit, below which no fatigue failures would be expected. However, non-ferrous metals do not typically exhibit a fatigue limit. Instead, decreased fatigue loads still will cause a fatigue failure, although it may be at a very large number of cycles.

strength. Since nonferrous-based alloys do not exhibit an endurance limit, a fatigue strength is often calculated to allow comparison to other materials, including ferrous-based alloys. The fatigue strength is defined as the stress amplitude to cause failure in 10^7–10^8 cycles normalized by dividing by the ultimate tensile strength. In some cases, the fatigue strength is also called the fatigue ratio. In ferrous-based alloys, the fatigue strength is the endurance limit divided by the ultimate tensile strength. Nonferrous systems, such as Ni-base, Cu-base, and Mg-base systems, can exhibit fatigue strengths of about 0.35. Note that the fatigue strength should not be considered a material constant, but is a convenient tool for comparison of different materials when tested under similar conditions. Another ratio used to compare materials is the notch sensitivity ratio, in which the stress range to cause failure at some given cyclic lifetime is compared between notched and unnotched (or smooth gage) samples. When the ratio is less than one, the material exhibits a reduction in fatigue strength in the presence of a stress concentrator (ie, the notch). Notch strengthening is observed when the ratio is greater than one. In most cases, though, the presence of a stress concentrator results in significantly reduced fatigue strength.

Since, as noted above, fatigue strength is typically correlated with the tensile strength of a material, increases in tensile properties will frequently result in increased fatigue resistance. However, the increases observed in fatigue strength due to increased tensile properties are typically not proportional. Materials that exhibit high tensile strength do not, therefore, necessarily exhibit high fatigue strength. There are some general trends, though, that can be observed between fatigue and tensile strengths. In general, increased strengths from refinement of the microstructure and solid solution strengthening result in increased fatigue strength. For example, refinement of the grain size results in increased tensile and fatigue strengths. On the other hand, increased strength from precipitation hardening or coarsened microstructures frequently result in decreased fatigue strength. Typically, metallurgical modifications that result in more uniform or homogeneous plastic deformation will result in increased fatigue strength. In addition, the stacking fault energy (SFE) determines the difficulty of cross-slip of dislocations during deformation. Materials with high SFE will exhibit cross-slip more easily, which can result in the formation of slip bands (ie, less homogeneous deformation) and decreased fatigue strength. High SFE materials are said to exhibit wavy slip; whereas, planar slip is observed in low SFE materials which do not exhibit much cross-slip. The presence of inclusions can also result in reduced fatigue resistance due to stress concentration and the effect of the particles on slip.

Sample Size and Surface Finish. There is a strong influence of sample size on the fatigue performance of a material. In general, larger samples exhibit lower fatigue strengths than small samples. The differences may stem from the differences in metallurgical structure, residual stress distribution through the cross-section, surface area-to-volume ratio, and possible sensitivity to defects which may be more frequent in larger samples. Since fatigue failures often start at the surface the surface area-to-volume ratio may be a significant factor in the differences. However, not all materials exhibit a size effect in the fatigue properties, so care must be taken when using fatigue data generated on small samples when designing a large component.

The surface finish and condition have significant impacts on the fatigue properties of a material. In many types of fatigue loading, torsion and bending for example, the maximum stresses occur at the samples surface. So it is not surprising that fatigue failures in this type of testing occur at the sample surface. However, surface initiation of fatigue failures frequently occurs in axial loading, as well. The primary reasons that fatigue failures initiate at the surface include surface roughness or stress risers, changes in the fatigue strength at the surface of a material, and changes in the residual stresses at the surface. In addition, corrosion and, at high temperature, oxidation of the surface material may also contribute to the surface fatigue failures. The surface roughness can have a profound effect on the fatigue properties of a material, since any remaining machining marks, scratches, or defects will act as a stress riser to initiate the fatigue failure. Smoother surface finishes, by mechanical and electro-chemical polishing will result in significantly longer fatigue lives. The surface condition, including the local composition or microstructure, may also result in reduced fatigue properties. Lastly, residual stresses at the surface can either increase or decrease the fatigue resistance of a material. Compressive residual stress, from shot-peening, for example, will result in significantly increased fatigue resistance. However, residual tensile stresses will reduce the fatigue resistance.

Effects of Temperature. Temperature can have a significant impact on the fatigue resistance of a material. In general, decreasing the test temperature below room temperature results in increased fatigue resistance. At temperatures below the ductile brittle transition temperature (or DBTT), some ferrous-based alloys exhibit increased notch sensitivity, but do not seem to exhibit any significant reductions in fatigue properties. Similar to the effect of strengthening on the fatigue properties, as discussed above, a decrease in the test temperature has a greater effect on the tensile properties than the fatigue properties.

Increasing the test temperature above room temperature, generally, results in decreased fatigue resistance. Some materials will exhibit an initial increase in fatigue strength, followed by a decrease in fatigue resistance, with increasing temperature. This increase in fatigue strength occurs in a temperature range in which an increase ultimate tensile strength is observed. However, the mechanism for this anomalous increase in fatigue strength is not completely understood. Further increases in temperatures above approximately half of the homologous temperature (= Test Temperature/Melting or Solidus Temperature), results in an further reduction in the fatigue resistance that may be due to creep damage. As the test temperature increases further, the failure mechanism can shift from fatigue failure to creep failure, with a concurrent change in fracture. Fatigue failures are frequently transgranular; whereas, creep failures are frequently intergranular. In general, increased test temperatures and/or increased stress levels, will result in increased amounts of creep and decreased fatigue resistance. This reduction in fatigue life, due to the combination of creep and fatigue loading is called creep-fatigue interaction.

Increased test temperatures also can result in significant environmental interactions. The grain boundaries in polycrystalline materials can exhibit local oxidation, ultimately resulting in crack initiation and/or propagation. General oxidation and selective oxidation of one or more phases at the sample surface can also lead to significant reductions in fatigue resistance. Internal oxidation

can occur in samples due to rapid diffusion of oxygen down grain boundaries and/or if nonprotective oxides form on the sample surface. The higher test temperatures result in more rapid diffusion rates which will result in increased reactions with the environment.

Lastly, increased test temperatures can result in creep-fatigue-environmental interactions, due to the reaction of the test material with the environment and the combination of creep and fatigue loading. Generally, the creep-fatigue-environment interactions result in significantly reduced fatigue strength. As noted above, this interaction typically does not occur until the test temperatures are in excess of about half the homologous temperature. Some of the degradation in fatigue properties due to the effects of the test environment and temperature have been correlated with a frequency effect. At higher frequencies, the fatigue life is independent of the frequency and failure occurs by the usual transgranular mechanism. At lower frequencies, the fatigue life is dependent on the frequency due to interactions with the environment and due to creep effects. The failure mechanisms also change due to the environmental and creep interactions from transgranular to intergranular. Similar transitions can be observed when unique waveforms are used which impose a tensile hold at the maximum stress/strain.

When testing under isothermal, or constant temperature, conditions, the fatigue resistance of a material is generally decreased. However, all of the stresses/strains that cause fatigue are not from mechanical sources. Fatigue can also be caused by temperature variations. Thermal stresses result from the constraint of changes in dimensions of a component due to thermal expansion/contraction from temperature changes. The constraint can result from the structure around the component or from temperature differences within the component. The thermal stresses developed by temperature differences or changes (ΔT) within a component are:

$$\sigma = \alpha E \Delta T$$

where α = linear thermal coefficient of expansion and

E = elastic modulus.

Materials within limited ductilities and low thermal conductivities are subject to thermal fatigue. In order to decrease the effect of thermal fatigue, the temperature difference (ΔT) must be decreased, the modulus must be reduced (for example in single crystal Ni-base superalloys) or the coefficient of thermal expansion (α) must be reduced.

In some cases, materials are subjected to both thermal and load/strain variations simultaneously. The super-position of thermal fatigue with strain/stress controlled fatigue testing is often referred to as thermo-mechanical fatigue (TMF). In most cases, the temperature cycles are out-of-phase with the strain cycles, in order to cause the material to contract due to cooling while tensile strains are being applied. This condition is the most severe test for the material.

Effects of Stress/Strain Range and Waveform. Increasing the strain or stain range results in reduced fatigue life whether the test is to determine the number of cycles to crack initiation or failure or to measure the fatigue crack growth rate. In addition, the mean stress/strain and the R-ratio have a signifi-

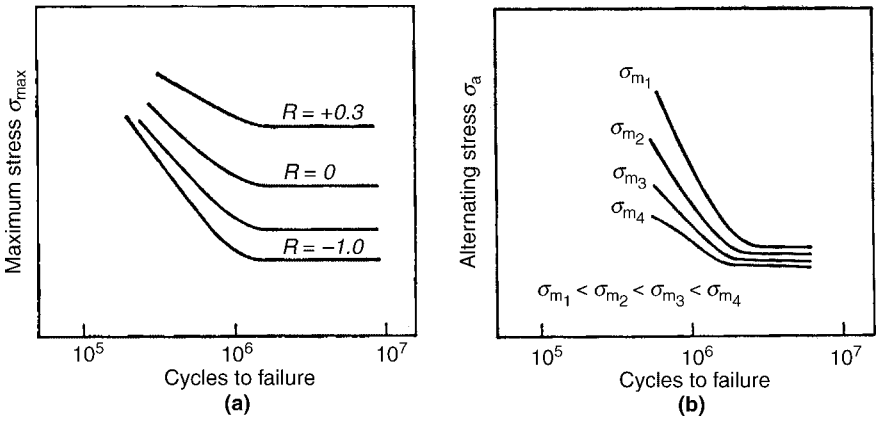

Fig. 11. The effect of mean stress on the fatigue resistance of a material is illustrated in the Goodman diagram above. Note that an increase in the mean stress, results in a reduction in the stress range to cause failure.

cant impact on the fatigue properties of a material. In general, increasing the mean stress/strain while holding the alternating stress/strain constant results in a significant decrease in fatigue life. Increasing the mean stress results in increased maximum and minimum stresses which result in reduced fatigue life. Similarly, decreasing the R-ratio, while holding the maximum stress/strain constant results in a greater alternating stress/strain range and, therefore, reduced fatigue life. In the extreme case, when $R = -1.0$, the test is considered a fully reversed fatigue test. The effects of mean stress on the fatigue life have been represented by Goodman diagrams (Fig. 11) which plot the maximum and minimum stresses that cause failure as a function of mean stress.

3.2. Practical Aspects of Fatigue Property Characterization. There are three primary types of fatigue testing; high cycle fatigue, low cycle fatigue and fatigue crack growth rate testing. Each type of testing addresses a unique aspect of fatigue and will be discussed separately below.

The Basic Fatigue Test. A fatigue test imposes a cyclic load or displacement on a sample at a given temperature (18–24). The load/displacement can be applied by mechanical means or by thermal gradients. The cycles of the applied load/displacement are counted to determine the number of cycles to crack initiation, cycles to failure and the growth rate of the fatigue crack. The load/displacement is usually applied in a uniaxial manner along the length of the sample by a servo-hydraulic or electro-mechanical test system (Fig. 12). Other systems which have been used to apply the load are torsion systems, rotating beam and multiaxial test systems. As noted previously, there are three basic types of fatigue tests: high cycle fatigue (HCF), low cycle fatigue (LCF) and fatigue crack growth rate (FCGR) testing.

The Basics of High Cycle Fatigue Testing. High cycle fatigue tests are usually performed in load control in which the maximum and minimum loads are selected based on the stress amplitude. The desired load waveform is then applied to the sample and measured by a load cell in the test frame. In most

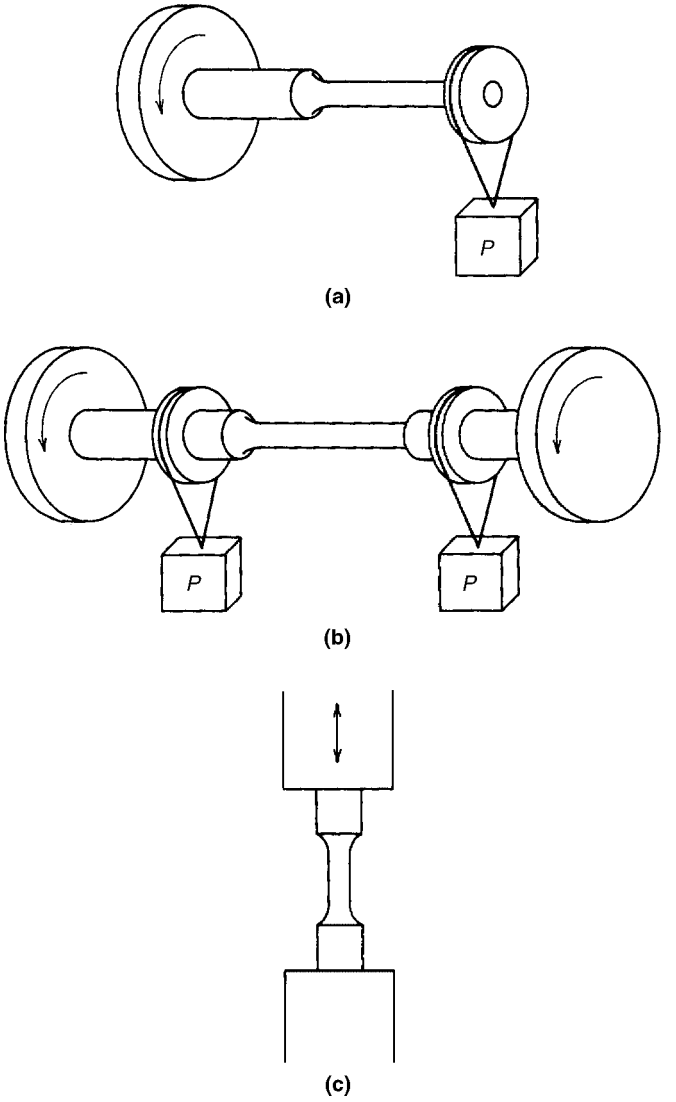

Fig. 12. Various types of sample loading typically used for fatigue testing. Single point (**a**) and double point (**b**) bending is used for fully reversed fatigue testing. Axial loading (**c**) can be used for all types of fatigue loading waveforms.

cases, no attempt is made to measure the strain or the crack growth rate. The sample is cycle until failure occurs or until the test is stopped and the samples is considered a run-out. In general, high cycle fatigue tests last between 10,000 cycles and 10,000,000 cycles. Most testing is performed a frequencies in the range of 20–50 Hz. Therefore, the high cycle fatigue tests that run up to 10^7 cycles, which are considered run-outs, take about one week to complete when run at 20 Hz. Run-out samples are not tested further or, in some cases, the stress amplitudes are increased and the sample is put back into test. However, care

must be taken when using data from these run-out samples at increased stress amplitude since they previous 10^7 cycles may have an influence on the subsequent fatigue properties.

In most cases, either a triangular or sinusoidal waveform are used in most testing conditions. Rarely are tensile holds performed to evaluate the effect of creep or environmental interactions. In most cases, the R-ratio, frequency or mean stress are changed in to determine the environment and creep components in the fatigue behavior. In general, most of the HCF testing is performed on cylindrical test samples with either button-head loading or threaded ends. However, plate samples or other geometries can be utilized for HCF testing, as well.

Once the sample has failed, fracture surfaces are carefully examined optically and then using scanning electron microscopy. The fatigue crack initiation site is determined and the crack growth behavior is observed. In some cases, fatigue striations can be observed which represent the step-by-step growth of the fatigue crack. Lastly, the overload when the sample ultimately fails is also characterized. Transmission electron microscopy (tem) is also frequently performed to evaluate deformation mechanisms.

High cycle fatigue testing can also be done using ultrasonic fatigue testing, where very high cyclic frequencies are used. Frequencies greater that 1 KHz are used and allow for testing to very high cycle to failure lifetimes within much shorter test times. However, there are significant limitations when performing ultrasonic fatigue testing and care must be taken to control test conditions to prevent changes in sample, such as sample heating and changes in deformation.

The Basics of Low Cycle Fatigue Testing. Low cycle fatigue testing is performed in strain or displacement control. When testing using strain control, the strain is measured by a extensometer applied to the samples directly or by an extensometer frame if testing at high temperature. The strain range is selected, with an R-ratio of -1.0, which indicates fully reversed testing. Although the test is controlled by monitoring the strain and/or displacement, the load, and, therefore, the stress, are also measured. The cyclic stress and the cyclic strain are plotted on a graph for each cycle during the test. An example cyclic/strain graph is shown in Figure 13. The width of the cyclic stress–strain curve indicates that amount of plastic deformation. The wider the cyclic stress–strain curve, the greater the plasticity of the applied wave form and, hence, the shorter the fatigue life (Fig. 6). These cyclic stress–strain curves are also useful to determine when fatigue crack initiation has occurred. Since the test is performed in strain control, the maximum and minimum strains of the applied waveform is held constant. However, the load can vary. During a typical test, the load can either continuously increase if the sample cyclically hardens or decrease if cyclic softening occurs (Fig. 14). When a crack forms, the tensile load bearing capability of the material is decreased since the cross-sectional area of the sample decreases as the crack forms and grows. Note that when the cyclic hardening or softening occurs, both the maximum and minimum stresses will change. When a crack forms, though, only the tensile side of the cyclic stress–strain curve will change.

In most cases, either a triangular or sinusoidal waveform are used in most testing conditions. However, in order to evaluate the effect of elevated temperatures, tensile holds can be used at the maximum stress. These holds, as noted previously, will highlight the effect of environment and creep in the fatigue

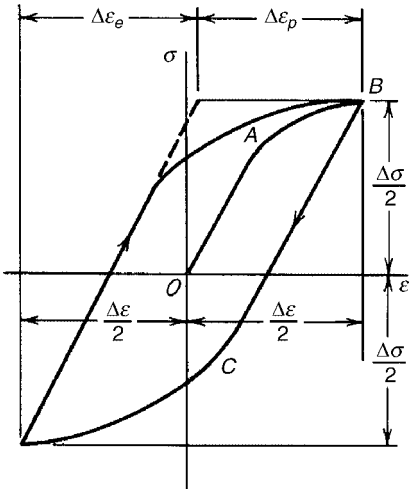

Fig. 13. Schematic of cyclic stress-strain loop during a strain-controlled fatigue (LCF) test. Note that there is both an elastic portion ($\Delta\epsilon_e$) and a plastic portion ($\Delta\epsilon_p$) of the loop. Generally, the greater the plastic portion of the loop, the shorter the fatigue life.

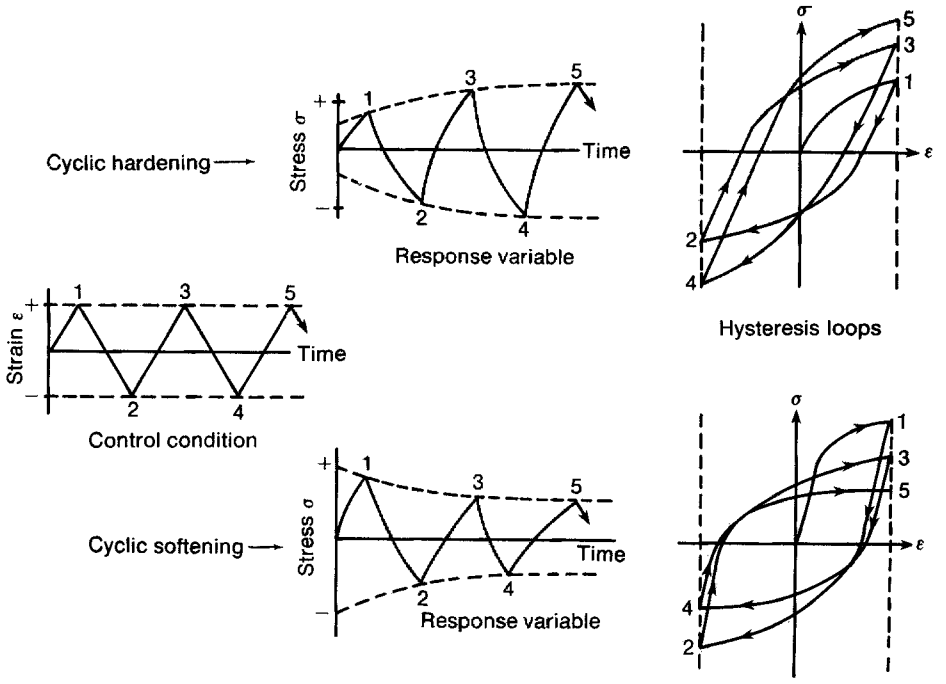

Fig. 14. Schematic representation of cyclic hardening and cyclic softening that can occur during strain controlled (LCF) fatigue testing.

properties. In general, most LCF testing utilizes cylindrical test samples with either button-head loading or threaded ends. In some cases, plate samples can also be utilized, but since most LCF testing is fully reversed, the cross-sectional area of the samples must be sufficient to support the compressive load and not buckle.

Most LCF testing is performed in the frequency range of 0.1–20 Hz, with 0.33 Hz the most commonly used frequency. At these relatively low frequency, typical sample lifetimes are 1,000 to 100,000 cycles to failure. If samples last longer than the indicated 10^6 cycles, frequently the test is changed from an LCF test to a HCF test by changing the control mode from strain control to load control. The resulting HCF test is then run until 10^7 cycles at much higher cyclic rates.

Similar to the HCF testing, once the sample has failed the fracture surface is completely characterized by optical and SEM techniques. Transmission electron microscopy (tem) is also frequently performed to evaluate deformation mechanisms.

Basics of Fatigue Crack Growth Rate Testing. Similar to HCF testing, the fatigue crack growth rate testing is performed in load control in order to control the stress intensity at the crack tip. In FCGR testing, a crack is grown in the material and the rate at which the crack advances under cyclic loading is measured (Fig. 8). The crack initiation event is not important. A fatigue crack is preferred over a machined notch, since the stress concentration factor is much greater for a sharp fatigue crack and there are no complications from residual stresses from machining. Once the initial crack is grown into the test samples, the crack length is measured and the test started. Under the stress controlled waveform is applied to the sample, the crack grows in length, slowly at first and then at a faster rate as the crack grows. In general, the crack growth rate is increased at higher stress amplitude (ie, stress intensity). In addition, increased test temperatures will also result in more rapid crack growth rates.

In most cases, either a triangular or sinusoidal waveform are used in most testing conditions. However, in order to evaluate the effect of elevated temperatures, tensile holds can be used at the maximum stress. These holds, as noted previously, will highlight the effects of environment and creep on the fatigue properties.

Some of the techniques used to measure fatigue crack growth include a traveling optical microscope, electric potential drop methods, crack opening displacement or compliance techniques. Elevated temperature testing may require modification to these techniques. The crack length is then correlated to determine the crack growth rate (da/dn) as a function of the crack length, and the stress intensity factor at the crack tip. Numerous sample geometries are used for FCGR testing, but the most common are compact tension samples, single edge notched and center notched. All of these samples have in common a machined notch, from which a fatigue precrack is grown prior to starting the tests. Most samples have a single crack growing from a side, but some samples will have a crack at the center of the sample with two growing crack fronts.

The fatigue crack growth test is usually also run at 20 Hz, but requires samples precracking and sample preparation and typically take up 2 days to run. Most fatigue crack growth tests, though, are easily completed within a day.

Similar to the HCF and LCF testing, once the sample has failed the fracture surface is completely characterized by optical and SEM techniques.

Environment. As noted previously, the environment can have a profound effect on the fatigue properties of a material. At low temperatures, the presence of a corrosive environment, which can include high purity water, can result in significant high fatigue crack growth rates and shorter fatigue lives. This type of fatigue is referred to as corrosion fatigue and is commonly evaluated in steels used for pressure vessels and materials for steam generators and nuclear reactors. At elevated temperature, there can be an interaction between sustained tensile loads and oxidation/corrosion referred to as creep-fatigue environment interaction. Typically, this behavior is a concern for materials used for gas turbines, such as turbine disks, blades and vanes. When testing materials to determine if these types of environmental interactions can occur, it is important to ensure that the desired test environment is actually present at the crack and that no interactions with the furnace, chamber, grips, fixtures, etc alter the environment. In addition, it is necessary to ensure that the grips and pull-rods are capable at the temperature in the test environment for the testing duration. Lastly, it is important to note that more complexity is necessary to perform test to evaluate temperature–environment effects on fatigue properties. This increased complexity is accompanied by a significant increase in difficulty and, therefore, cost.

3.3. Fatigue Data Analysis and Potential Problems. Regardless of the material, fatigue failures will occur when the components are exposed to cyclic stress, strains, temperatures or any combination of thereof. Since a very large proportion of engineering failures are related at least in part to fatigue, it is very important to consider the cyclic behavior of materials being considered for an application. However, there is no single method to evaluate the fatigue properties of a material. The ultimate use, service environment, intended lifetime, cost, and cost of failure must be considered when developing the test plan.

There is a substantial database on the fatigue properties on a wide variety of engineering materials. Numerous compilations of the fatigue data have been published and the material developer/processor may also be able to provide valuable information. Since there is such a large potential for scatter in fatigue data, extreme care must be used when utilizing data from the literature and comparing any recently obtained data with that literature data. Techniques have been developed for presentation of fatigue data and comparison of various sets of data (18–22).

However, it is especially important to develop a significant amount of data prior to attempting to develop an S-N, ϵ-N or da/dN vs ΔK curve. It should be noted, that in most cases, the fatigue data are represented as a deterministic plot where given a stress amplitude, for example, the number of cycles to failure can be determined. However, the determined number of cycles to failure is the average or mean number of cycles to failure (Fig. 9). In most cases, several samples (eg, at least 6) are tested at each condition to develop the appropriate statistical database. In addition, having a database with numerous samples tested at each condition, will allow for the development of a probabilistic relationship. For more complex designs, it is essential to develop the probabilistic fatigue behavior of a material. Often times, mechanical engineers and designers will require the data and the scatter to produce the probabilistic relationship.

When comparing fatigue data it is necessary to ensure that the materials have been processed in a similar manner to obtain the appropriate microstructures, prepared in similar manners and test under very similar conditions. As seen previously, changes in the R-ratio or the mean stress (σ_{mean}) can results in significantly different fatigue properties. In addition, the frequency or wave-type used for testing can also have an impact on the fatigue properties. Therefore, comparison of fatigue data can only be done with any accuracy if, the test conditions are very similar.

Most HCF data are presented in an S-N curve and ϵ-N curves are used to plot LCF properties. The fatigue crack growth rate testing almost always plotted as a da/dN versus ΔK. Although empirical relationships have been developed to convert various forms of fatigue properties, these relationships on only applicable to a few alloys used to develop them. Trying to apply these empirical rules to other materials systems often yields inaccurate data.

Representation and comparison of fatigue data generated either at high temperature or in aggressive environments can result in additional difficulties. Reaction of the test materials with the environment, due to oxidation at high temperature or corrosion can result in the formation of a surface scale on the crack surface. This scale can effective act as a wedge in between the fracture surfaces, effectively preventing the crack from fully closing. When the fatigue crack can not fully close, the effective stress cycle being placed on the sample is reduced. This phenomenon is referred to as crack closure and, if it occurs, it the fatigue data must be manipulated to account for the reduced stress cycle.

4. High Temperature Alloy Design: Strengthening Mechanisms

As previously discussed, some elements make better candidates for high temperature materials applications. However, most elements do not exhibit a reasonable balance of engineering properties to allow them to be selected for structural applications. Therefore, the elements that can be considered for elevated temperature applications must be alloyed with the appropriate element to increase the strength, creep resistance, fatigue resistance, environmental resistance and/or processability.

For a material to be a useful engineering material it must posses a balance of properties. The most common properties that are to be used for selection of a material are tensile (monotonic), creep (or time dependent) and fatigue properties. The candidate material must exhibit sufficient resistance to deformation for a given component lifetime at stresses determined for the application. In addition, the effect of the environment on the properties is also a concern for high temperature applications.

4.1. Tensile Strengthening. Similar to "low" temperature applications, adequate tensile strength is necessary for elevated temperature service. Both high and low temperature applications can benefit from increased tensile strength. In general, it is well know that metals deform by the motion of a dislocation under the influence of a shear stress. An increase in strength of a metal is observed when the generation and motion of dislocations becomes more difficult. However, it should be noted, though, completely preventing the generation

and motion of dislocation is not desirable, since this would result in a material with degraded properties (ie, fatigue and toughness). Methods to increase the tensile strength are discussed below.

Cold Work. One of the simplest ways to increase the strength of a material is to the cold work the sample. Deformation processing at temperatures below the dynamic recover/recrystallization temperature results in a significant increase in the dislocation density. This increased dislocation density results in significantly higher flow stresses due to the extensive amount of dislocation interaction, which impedes dislocation motion. The increased flow stress is generally accompanied by a decrease in ductility. However, as the temperature is increased, a cold worked material will start to go through recovery and recrystallization processes (Fig. 15). The resulting material will have a finer grain size than the starting material, with a lower strength, but higher ductility than the cold worked material. If the sample is held for a longer time, the grain size of the sample will increase resulting in a further reduction in strength and ductility.

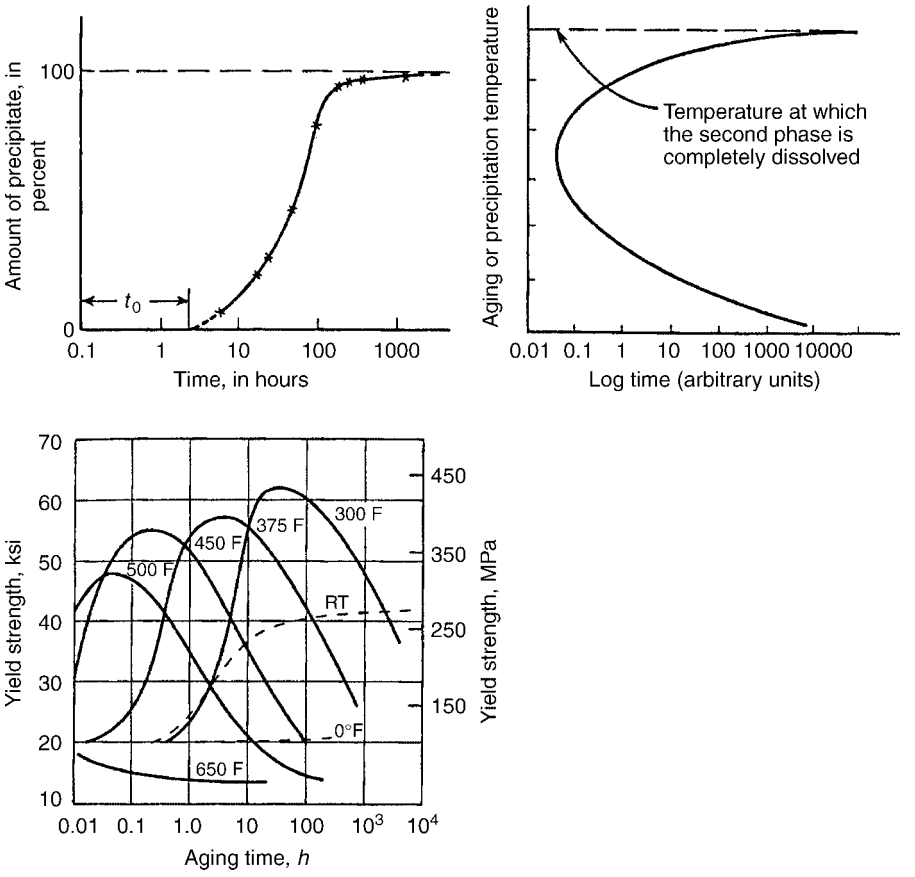

Fig. 15. Effect of aging temperature on the precipitation hardening reaction of Al alloy 2014. Note that during aging, there is an incubation period (t_0) before the amount of precipitation, and the strength of the alloy, increases. As the aging temperature increases, the time to reach the peak strength is decreased.

Grain Size Effects. Another simple way to increase strength of a material is to decrease the grain size, usually by deformation processing. The Hall-Petch relationship (ie, $\sigma = \sigma_0 + kd^{-1/2}$) indicates that the strength is inversely related to the square-root of the grain size (d). Decreasing the grain size by repeated cold working and recrystallization can result in a significant increase in strength and ductility. The finer grain size have shorter slip distances, which means small dislocation pile-ups at obstacles, such as grain boundaries. Since these dislocation pile-ups are shorter, and therefore have lower stresses acting at the obstacle, it takes additional stresses to propagate slip beyond the obstacle. Reduction of the grain size is one of the few methods to increase the strength without decreasing the ductility. Note, that this technique would be expected to increase the fatigue resistance, but may not be useful for increasing the creep resistance of a material. The higher tensile strength of the finer-grained material will still be observed at high temperature, but it will also result in dramatically reduced creep strength. At higher temperatures, the grain boundaries are weakened and grain boundary sliding will occur. This type of deformation will not be obvious at high strain rates, but during creep rates it will be obvious. Frequently, the high ductility of the fine-grained material can be used to produce superplasticity. However, for high temperature strength and creep resistance, fine grain size is not desirable.

Alloying, Substitutional Solid Solutions. In substitutional solid solutions, the solute atoms occupies the solvent atom lattice sites. The solute atoms are typically similar in size, compared to the solvent atoms. In general, the more similar the solute and solvent atoms, the greater the solubility, as noted by the Hume-Rothery rules. Although Ni is not endowed with a distinctly high modulus of elasticity or low diffusivity, Ni has a high tolerance for alloying without phase instability and has the tendency to form a protective surface oxide when alloyed with Cr or Al. The effectiveness of the strengthening from the addition of the solute atom can be evaluated by considering the solubility of solute in the solvent and the rate of hardening for the solute. In general, the substitutional atom produces a relative strengthening of about 1/10 of the solute atom.

As the valence difference between the solute and the solvent atom increases, the solid solubility decreases. The valence difference determines the e/a-ratio (the electron-atom ratio) which helps to determine stability. Significant changes to the e/a-ratio can result in structures becoming unstable or cause a transformation to a lower energy structure.

When considering the strengthening effect from the addition of the solute atom, the source of the strength is generally attributed to lattice misfit, modulus misfit, order, stacking fault interactions and electrical interactions (25–29). The strength of the alloy as been observed to increase with increasing size difference of the solute and solvent atoms and/or the resulting lattice parameter. The differences in the sizes of the solute and solvent atoms results in strengthening effects due to the interactions with dislocations. If the diameter of the substitutional solute atom is different than that of the solvent atom, the lattice is strained. A larger solute atom expands the solvent lattice, while a smaller atom contracts it. The lattice distortion associated with a substitutional atom is assumed to be spherical (dilational) and, therefore, strongly interacts with screw dislocation and, to a lesser extent, edge dislocations. The strains associated

with the substitutional solute atom can be relieved by interactions with the dislocations.

The misfit strengthening, sometimes referred to as elastic interactions, occurs between the elastic strain fields surrounding the misfitting solute atom and the core of a dislocation. The relative size or misfit factor is typically:

$$\varepsilon = 1/C(\Delta a/a0)$$

where Δa is the difference between the lattice parameter of the pure matrix, a_0, and the lattice parameter of the solute atom. The lattice misfit, ε, is measured by unit solute concentration, C. The strengthening is directly proportional to the misfit of the solute,

$$\tau = 2G\epsilon C.$$

Where τ is the yield stress for a dilute solid solution, G is the shear modulus, ε is the size misfit and C is the concentration of the solute atom. It has been shown that although the strengthening effects of solid solutions are usually overestimated by these predictions, the solid solution strengthening persist to temperatures of at least 0.6 T_m (where T_m is the homologous melting temperature), which is about 815°C.

Alloying, Interstitial Solid Solutions. In interstitial solid solutions, the solute atoms are much smaller (usually <0.65x(solvent atom)) and occupy the interstitial sites. The interstitial atoms most commonly observed in most metals are B, C, N, H, and O. Interstitial solute atoms produce a nonspherical lattice distortion and produce a strengthening equivalent to three times the shear modulus of the solute atom. Since the interstitial solute atoms exhibit both dilatational and shear components, it can interact with both screw and edge dislocations. Similar to substitutional solid solution strengthening, the interstitial solid solution strengthening is also effective up to at least 0.6 T_m.

Modulus Misfit Strengthening. A modulus interaction occurs if the presence of a solute atom locally alters the modulus of the lattice. Softening is observed locally if the solute atom has a smaller modulus which results in a reduction in the strain field of a dislocation. Therefore, the dislocation will be attracted by the solute atom, which will reduce the mobility of the dislocation. A repulsion of the dislocation and the solute atom is observed in the solute atom is observed if the solute atom has a greater shear modulus, which results in local hardening of the lattice and an increase in the strain field. Although the modulus misfit strengthening is similar to the size misfit, both screw and edge dislocations are effected by the modulus misfit strengthening. A change in the shear modulus is accompanied by a local change in the bulk modulus, therefore, both screw and edge dislocations are affected.

Fleischer suggested that the modulus difference between solute and solvent may give rise to strengthening due to the extra work needed to force a dislocation through hard or soft regions in the matrix (25). Fleischer also suggested that the modulus difference and the lattice misfit can be incorporated into a single relationship. However, this relationship does still overestimate the strength of a solid solution, and may not be applicable to alloy systems.

Stacking Fault Interactions. Stacking fault interactions are also sometimes referred to as chemical strengthening and are due to the preferential

segregation of solute atoms to the stacking faults in extended dislocations (27). For this mechanism to occur, the solute atom must have a preferential or increased solubility in the HCP structure of the FCC stacking fault. As the concentration of the solute within the stacking fault increases, the SFE decreases, which results in a further increase in the separation of the partial dislocations. Therefore, the motion of the dislocations is made more difficult and additional work must be done to constrict the pair of dislocations. The stacking fault interactions would be considered to be a viable mechanism at both low and high temperatures, however, the contribution at any temperature would likely be relatively small.

Short Range Order (SRO) Hardening. Solute atoms that tend to arrange themselves so that they can maximize the number of dissimilar nearest neighbors, results in the formation of short range order or SRO. Strengthening occurs since the motion of a dislocation through a region of SRO will result in a reduction in the degree of SRO. This local disordering will cause an increase in the energy of the alloy and, therefore, it is not energetically favorable for the dislocation to move through the region of SRO.

SRO can be observed in concentrated solid solution alloys. The energy required to shear a short range lattice causes an increase in the flow stress for the alloy. Ni-Cr alloys in the vicinity of 20–25 wt% Cr can exhibit SRO after long-term aging at temperatures below about 500°C. Typically, the alloys developed for oxidation/corrosion resistance have compositions with high levels of Cr. In addition, alloys developed for industrial gas turbines (IGT) applications have relatively high levels of Cr for increased resistance to hot corrosion. In addition, alloys with higher levels of γ' volume fractions typically have low levels of Cr. However, Cr tends to partition to the γ matrix and the levels of Cr than accumulate in the γ can approach those necessary to exhibit SRO.

Long Range Ordering (LRO) Hardening. Long range order, or LRO, hardening occurs in alloys that exhibit a superlattice. Some alloys exhibit LRO when their composition is a distinct atom ratio (ie, AB, A_3B, etc), and when it is thermodynamically favorable, below some critical temperature (T_c) for specific atoms occupy specific lattice sites. In a superlattice, there is a long-range periodic arrangement of dissimilar atoms. The movement of dislocations through the superlattice creates a region of disorder called an antiphase boundary (APB), because the atoms across the slip plane has become "out of phase" with respect to the energetically preferred superlattice. This local "dis-order" is the APB, and in order to minimize the energy to create the APB, a second dislocation follows the first dislocation and re-creates order in its wake. The combined dislocations with the APB are called a super lattice dislocation or a superdislocation. The stress required to move a dislocation through a region of long range order is proportional to the APB energy and inversely related to the spacing of the dislocations. As deformation occurs, more APB's are formed, reducing the spacing, and causing greater dislocation–dislocation interaction, and results in increased hardening. Typically, ordered alloys exhibit much higher work hardening rates from cold work than disordered alloys, but the yield strength of the ordered alloys is often times lower than disordered alloys. However, the fatigue strength of the ordered alloys is typically very high due to the planar slip and slowed diffusion resulting from the ordered lattice. The ductility of most ordered alloys,

though, is reduced due to the presence of the ordered lattice reducing the number of active slip systems. Therefore, ordered alloys frequently exhibit limited ductility and are brittle at low temperatures but exhibit increased ductility at higher test temperatures (when other slip systems become active or thermally activated cross-slip/climb occurs).

4.2. Precipitation Hardening. Since only a few alloy systems permit extensive solid solubility between two or more elements and these systems exhibit only a moderate level of solid solution hardening, most commercial alloys contain a heterogeneous microstructure consisting of two or more phases. Although these phases can be present at a wide variety of morphologies, the vast majority of microstructures fall into two classes. The two phases can be present in discrete grains, sometimes referred to as the aggregated type of two phase microstructure in which the second phase is of the order of a grain size of the matrix. This type of microstructure is seen in alpha brass, alpha-beta Ti alloys and ferrite and pearlite colonies in a ferrite matrix in annealed steel. The other general category of two phase microstructures is when the second phase is much finer and is dispersed throughout the matrix. The second phase is generally much finer and may approach nanoscale size during the early stages of precipitation.

The strengthening from precipitation of a second phase is usually additive to the solid solution strengthening discussed previously. Alloys that are two-phase alloys produced by heat treatment, ensure a maximum solid strengthening component, since the precipitates form from supersaturated solid solution. In addition, the presence of the second phase particles in the matrix results in internal stresses which modify the deformation of the matrix. Several factors regarding the precipitates must be considered when describing the strengthening from precipitates. The factors most often used to describe precipitates include size, shape, number and distribution of the second phase particles, the strength, ductility and strain hardening behavior of the matrix and second phases, crystallographic fit between the phases and the interfacial energy and interfacial bonding between the phases. It should be noted that this is not possible to control each variable independently and it is not possible to measure each of these attributes with any degree of precision.

The deformation of the two-phase alloys with two ductile phases depends on the volume fraction of the two phases and the total deformation. Experiments have shown that not all second phase particles produce strengthening. In order for particle strengthening to occur there must be a strong particle-matrix bond. Deformation occurs first in the weaker phase, and if very little of the stronger phases is present, most of the deformation continues to occur in the softer phase. As deformation continues, flow of the softer matrix will occur around the particles of the harder phase. When the volume fraction is increased to about 30 volume %, or more, of the harder phase, the softer phase is no longer the completely continuous phase and the two phases tend to deform more or less with equal strains. At volume fractions of about 70 volume %, or more of the harder phase, the deformation is largely controlled by the properties of the harder phase.

Two-phase alloys with hard particles exhibit different deformation characteristics than the ductile phases above (30). However, the mechanical properties are dependent on the distribution of the second phase in the microstructure. If

the second phase is present as a continuous phase along grain boundaries, the alloy will exhibit low ductility. If, however, the second phase is not continuous, the brittleness of the alloy is reduced considerably.

Fine second phase particles distributed throughout the ductile matrix are commonly used to strengthen an alloy. There are two basic types of strengthening observed from precipitates. The first type is due to precipitation hardening and is usually produced by appropriate heat treatments. The second type of precipitation hardening is referred to as dispersion hardening and is attributed to the hardening of a matrix with hard, brittle, incoherent second phase particles.

The precipitation hardened materials frequently rely on a partial or full solution heat treatment to put the precipitates into solution and then reprecipitate them in the appropriate morphology and volume fraction in subsequent thermal or aging cycles. These second phase particles can be coherent and can produce significant strengthened when aged to the peak aged condition. The most widely used example system for precipitation hardening is the Al-Cu system. In the case of Ni-base superalloys, the precipitate is referred to as γ'-Ni_3Al and the matrix is the Ni-rich solid solution. The requirements for the precipitation reaction to be observed can be seen in the phase diagram. In general, precipitation can be observed in a system if there is a limited solid solubility for a second phase and if the solubility for the second phase decreases with decreasing temperature. The equilibrium morphology, composition and structure of the precipitates may not be the most desirable, in terms of mechanical properties. Often times, the best balance of properties can be attained with a fine distribution of precipitates that may exhibit a composition and structure that is quite different form the equilibrium phase. The aging heat treatments produce a range of precipitate sizes and compositions, producing an increasing strength with increasing aging heat treatment time (Fig. 15). The maximum in strength observed during heat treatment is often referred to as the peak-aged condition. The strengthening from these coherent precipitates is quite complex and usually attributed to coherency strains and antiphase boundary (APB) strengthening. The coherency strains result from lattice mismatch between the matrix and the precipitate. In general, as the size of the particle increases, the misfit, and, therefore, the strengthening from the precipitate, would be expected to increase. Furthermore, as the lattice mismatch increased, for example, due to alloying either the precipitate and/or the matrix, the strengthening from the precipitate would be expected to increase. However, a high degree of lattice mismatch would also be expected to result in a decrease in stability, and, therefore, an increase in the tendency and the rate for the precipitate to grow in size during heat treatment and during service. As the precipitate size increased, eventually the lattice mismatch can not be further increased and the precipitate would become incoherent. In addition, since the precipitates are often ordered, a dislocation cutting the particle would generate an APB and/or would have to be paired with a trailing dislocation to eliminate the APB. The strengthening from the ordered nature from the precipitate is related to the APB energy. In other words, an increase in strengthening would be observed if the APB energy was increased. In general, an increase in the APB energy would not be expected to result in more rapid coarsening or incoherency. However, if the size of the precipitate increased in size during service, the precipitate would likely become incoherent at some point,

resulting in a decrease in strengthening. In general, the very high strength, at all temperatures, of Ni-base superalloys is due to a combination of the misfit and order strengthening from the γ' phase, as well as the solid solution hardening of the γ matrix.

Continued aging heat treatments past the peak aged condition may produce the equilibrium precipitates with reduced strength, which is often referred to as over-aged. In many cases, the strengthening in the overaged condition is due to Orowan bowing mechanisms (30). The second type of precipitation strengthening is due to hard particles in a ductile matrix, usually referred to as dispersion hardening. Often time, these dispersoids are produced by mixing or blending of phases that are not soluble. The particles are generally, not coherent with the matrix and rely on Orowan bowing strengthening mechanisms. Dispersion strengthened materials generally can exhibit increased strength at high temperatures and can resist recrystallization and grain growth. Overaged precipitation strengthened alloys can also exhibit some strengthening due to Orowan bowing, but the strength of the overaged alloys is much lower than the peak-aged condition.

The dispersion hardening materials are frequently described as materials with ductile matrices, with hard second phase particles that are often brittle. The dispersion strengthened materials are frequently produced by mixing of powders or blending of powders, often by powder metallurgical techniques. The second phase particles are generally not soluble in or coherent with the matrix. Similar to the overaged precipitates discussed above, the strengthening observed in dispersion strengthened materials is usually attributed to Orowan bowing. The presence of the hard second phase particles can significantly increase the temperature for recrystallization and grain growth, and can produce a very thermally stale material. Since the phases can be blended, a wide variety of materials can be produced by mixing the desired matrix with the particles (which are usually oxides, nitrides, borides and carbides). In general, the strength of, dispersion strengthened alloys increases as the spacing between the particles decrease. Commercially available dispersion hardened alloys include the mechanically alloyed Fe- and Ni-base alloys (31). These materials typically have 2–3 volume % of 100–500A Y_2O_3 particles that are spaced approximately 500–3000A apart. The optimal strengthening from dispersion hardened alloys can be realized when microstructures with elongated grains are produced by directional processing and zone annealing. The strengthening derived from the dispersion hardening is also additive with the solid solution hardening, grain boundary hardening and precipitation hardening. In general, the dispersion hardening is not as effective as precipitation hardening, except at the very highest temperatures.

4.3. Composite Strengthening. In order to further increase the strength and temperature capability of high temperature materials, there has been a great deal of interest in the development of composite materials. In general, the matrix of these composites are relatively weak and the reinforcing phases are high strength, high modulus, but relatively brittle. By incorporating a second phase, in the form of fibers, lamellae or particulate, in a high temperature alloy matrix, a composite with increased capabilities may be developed. Similar techniques have been utilized to produce polymer–matrix and glass–matrix composites. However, the use of composites for high temperature applica-

tions has not yet been realized. Although the composite strengthening mechanism, similar to dispersion strengthening, offers the potential for strengthening at extremely high fractions of the melting point, the stability of the matrix/reinforcement interface and the chemical reaction between the matrix and the reinforcement, so far, has precluded the use of composite materials.

The incorporation of a strengthening phase into the composite can be achieved by creating the composite by combining the reinforcement and the matrix or by *in-situ* processing of two-phase materials with the second phase present as a fiber or a lamellae. The processing of these *in-situ* composites usually involves extremely slow directional solidification processes to form aligned structures. The deformation mechanisms of these *in-situ* composites is well documented and the strength the *in-situ* composites is at least comparable to the highest strength Ni-base superalloys. However, the cost of processing these materials is significantly greater than current materials, which has prevented these materials from being used in service.

4.4. Summary of Strengthening Mechanisms. In most structural high temperature alloys, several strengthening mechanisms are combined to produce a useful alloy (Table 1). Strengthening from only one or even two of the above mechanisms would not produce a useful balance of properties. For example, the precipitation hardened Ni-base superalloys all contain solutes that may produce significant amounts of solid solution hardening. So, the alloys that contain significant amounts of Al, Ti, Nb, and Ta to produce the γ' precipitates, also contain significant amount of W, Mo, Re and even some amount of the Al, Ti, Nb and Ta within the solubility limit provides some degree of solid solution strengthening. The Fe-base superalloys also contain similar types of elements for γ' precipitation combined with solid solution hardening. The Co-base superalloys utilize significant amounts of solid solution strengthening from Mo and W, as well as, extensive carbide precipitation for high temperature strength. In the extreme, there have been ODS alloys that rely on solid solution strengthening, dispersions hardening from Y_2O_3 and γ'-precipitation hardening. Obviously, high temperature alloys rely on several strengthening mechanisms to combine to form the highest strength alloys. How these strengthening mechanisms interact and sum to produce the strength observed in the alloys is not obvious. In many cases, the strengths are simplistically assumed to be additive. In a qualitative sense, this assumption is probably correct and many attempts have been made to develop technique to predict the strength of an

Table 1. **Strengthening Mechanisms for Both High Temperature and Low Temperature Applications**

Strengthening mechanism	Useful at low temperatures	Useful at high temperatures
cold work	yes	no
grain refinement	yes	no
solid solution alloying	yes	yes
precipitation hardening	yes	yes
long range ordering	yes	yes
dispersion strengthening	yes	yes
composite	yes	yes, if stable

alloy based on composition, phase stability and microstructure predictions from computational materials science techniques. However, most of these techniques are not successful in accurately predicting the strength of alloys outside very narrow compositional ranges. A significant amount of works remains to be completed before any model is developed that can predict the strength of the alloys.

5. Surface Stability and Environmental Resistance

Structural materials that are exposed to high temperatures must exhibit surface stability and resistance to the environment. In particular, when used in air, the material must resist oxidation and in combustion environments, the material must resist the attack of a variety of combustion by-products that can be very aggressive species, resulting in catastrophic failure. In general, the surface stability is described as resistance to oxidation and hot corrosion. In addition, the environmental resistance that is designed in high temperature structural materials can be achieved by alloying to the base metal and/or by using coatings.

5.1. Oxidation. When a metal is in contact with the environment at elevated temperatures, it will react to form a surface scale. If the environment contains oxygen, the scale that forms is usually an oxide and the formation of the oxide is called oxidation. In some cases, the oxide can be protective, slow growing and prevent further damage from the environmental interaction. However, in other cases, the scale or oxide that forms is not protective, fast growing and can even be in a gaseous form.

In order to achieve increased performance and increased efficiency, with decreased emission, the operating temperature of most power generating engineering systems has been driven to higher temperatures. This requirement for higher temperatures is often accompanied with the desire to used the materials at higher stresses (to reduce the systems weight or to reduce the stresses in other components) and to have longer component lifetimes (to decrease the total life-cycle cost of the system). The longer lifetime and higher operating temperatures requires an increasing oxidation and scaling resistance.

The oxidation damage to the material can take place under a variety of conditions and circumstances. The oxidation can take place in relatively inert environments, such as air, or in very aggressive environments, containing sulfur, halogens, and water vapor. Very rapid attacks, called hot corrosion, can be observed when condensed molten salts and oxidizing environments are present simultaneously.

Structural materials without sufficient environmental resistance can failure after a short period of time, as a result of rapid oxidation and/or hot corrosion, combined with rapid oxide growth and spallation. It has been shown that the adherence of the oxide can be dramatically altered by alloying and by control of impurities (ie, sulfur). Therefore, in addition to having an impact on strength, alloying of high temperature alloys, must also include the consideration of environmental resistance.

Surface Oxide Scale. As noted above, when a metal is exposed at high temperature, a surface oxide scale is formed. The scale morphology is dependent on the conditions of the reaction, the time of the oxidation, the composition of the

environment and the type and composition of the base metal alloy. Obviously, it is desirable to have a protective oxide that is adherent, fast forming, but slow growing and self-healing, if damaged. If the oxide is compact, in other words relatively thin and dense, it will be more protective than porous oxides which can not effectively inhibit the ingress of the aggressive species to the base metal. The oxidation rate is then determined by the chemical reaction at the surface of the metal at the base metal–oxide interface. If the oxide is compact and prevents the transport of the reactive species, then the oxidation rate is slow. However, if the oxide is porous, then the transport rate of the reactive species is not reduced and the oxidation rate is increased. At sufficiently high oxidation rates, due to poor protection by the oxide scale, the materials become inadequate for high temperature applications in anything but inert environments. In alloys with multiple alloying additions, multiple layers of oxide, some with complex compositions and with unique microstructures, can form. In order to achieve reasonable oxidation resistance in these alloys, it is necessary that at least one of the oxide layers must be compact and a slow growing oxide scale.

In most modern high temperature alloys, the environmental resistance is based on the formation of a slow growing, compact, chemically stable Cr_2O_3 or Al_2O_3, and to a lesser extent SiO_2 (32,33). These oxides grow much slower and more densely than to the oxides of the alloys bases (ie, Fe, Ni and Co) (34,35). The growth rate and protection of these oxide scales depends on the alloy content, temperature and environment. Generally, alloys contain high levels of either Al and/or Cr to form the protective oxide scale. At temperatures up to about 900–1000°C, Cr_2O_3 is very stable and resists oxidation and hot corrosion. At temperature above this level, though, Cr_2O_3 is not stable and volatilizes to a gaseous CrO_3, resulting in very rapid oxidation. At these higher temperatures, Al_2O_3 is the preferred oxide due to its stability and slow growing nature. However, in many cases, the Al content of the alloys is kept low to prevent the formation of the γ'-precipitate in solid solution alloys. For example, the Al content is limited in Fe-Al alloys since the ductility is observed to decrease with increasing Al content in these alloys. In addition, in hot corrosion atmosphere, Al_2O_3 scales are generally not considered protective, particularly in comparison to Cr_2O_3 scales.

The adherence of the oxide scale to the base metal is a major concern for elevated temperature service, particularly if thermal cycling of the material is expected. The coefficient of thermal expansion of the oxide is usually quiet different that that of the base metal. As the thickness of the oxide scale grows, the amount of mismatch in thermal expansion coefficient increases, resulting in an increase in the strains at the oxide/base-metal interface. These stresses will eventually result in the spallation of the oxide. If the oxide spalls off, the base metal will again be in contact with the oxidizing/corrosive environment, resulting in regrowth of the oxide scale. This cycle of oxide growth followed by spallation will result in a rapid and severe degree of oxidation damage. Generally, the material will start to exhibit a depletion of the oxide forming element(s) (eg, Cr and Al) in the near-surface region. In extreme cases, the near-surface layer depletion can result in a change in the type and composition of the surface scale when there is insufficient oxide former (ie, Cr and Al) present. If this happens, a faster growing and, often times, less protective oxide scale will grow. In

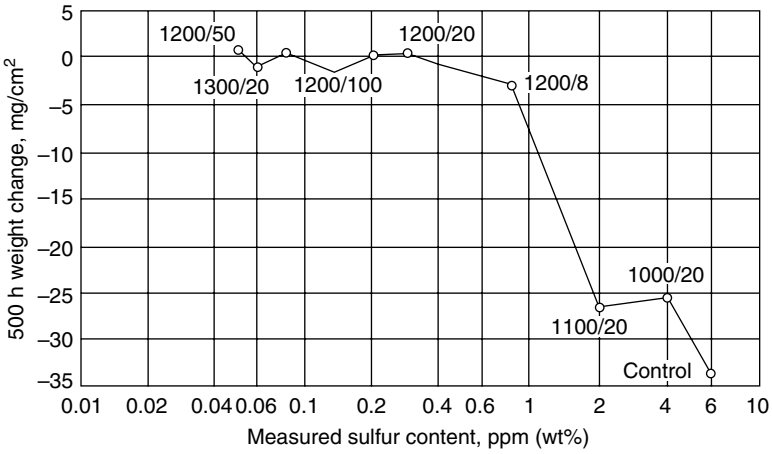

Fig. 16. The effect of S content on the 500h cyclic 1100°C oxidation resistance of PWA 1480. The samples were given various hydrogen anneals to remove S from the alloy. The figures indicate the temperature and time of these hydrogen anneals. Note that the baseline sample, indicated as control, contained 6 ppm wt% S. Increasing the temperature and/or time resulted in a significant reduction in the S content and a significant increase in the cyclic oxidation resistance of the alloy.

order to prevent this type of catastrophic oxidation damage, higher alloying levels of the oxide formers (ie, Cr and Al) can be utilized. However, care must be taken not to degrade other properties with excessively high levels of these alloying elements. Despite all of these drawbacks and the need to balance all types of properties, there are no current alternatives to the formation of protective Cr_2O_3 and Al_2O_3 surface scales.

Recent results, though, have indicated that the level of impurities has a profound effect on the oxidation resistance of Ni-base superalloy single crystals (34). It has been reported that reducing the sulfur level to below 1ppm wt% can significantly increase the oxidation resistance of Ni-base superalloy single crystals (Fig. 16). The sulfur can be removed by hydrogen heat treatments or by alloying (with rare earth elements, such as Ca). Similar results have also been observed in coating alloys. It is not clear if similar results would be observed in less highly alloyed, polycrystalline Ni-base alloys.

5.2. Hot Corrosion. The presence of molten salts on the surface of a component at elevated temperature, in addition to the oxidizing environment results in a more rapid attack of the materials called hot corrosion or sulfidation. The molten salt interacts with the oxygen in the environment, the surface oxide and the base metal to reduce the protective nature of the surface oxide scale. In severe cases, the surface oxide is essentially dissolved by the molten salt. The most common type of salt that is observed to cause hot corrosion is the Na_2SO_4. The presence of this salt on superalloys at high temperatures, such as those experienced in the first few stages of the turbine, results in hot corrosion (35). In general, the formation of the salt is attributed to the presence of impurities in the air (ie, NaCl or sea salt), fuel (ie, Na, V and S) and alloy (ie, S). These types of impurities are frequently present in marine or near-coastal applications

and when lower quality fuels, or coal-derived fuels are used. Whenever these impurities are present, the molten salts can be observed to form on the surface of the component. In addition, common alloying elements in the alloy, such as V, Mo and to a lesser degree W, can contribute to hot corrosion.

The morphology of the surface oxide and the reaction with the molten salt product is different than oxidation (36). The reaction between the oxide, base metal and molten salt often results in the formation of sulfur-type compounds below a porous oxide surface scale. These sulfide particles are often rich in Ni, Co and Cr. The depth and degree of hot corrosion damage is extremely variable and can be a function of temperature, environment and alloy content. In most cases, the corrosion rate reaches a maximum at 850–900°C and then decreases at higher and lower temperatures. At lower temperatures, the salt is solid and no hot corrosion is observed. At higher temperatures, oxidation is the primary concern, which indicates that the presence of the molten salt is required for this reaction to take place.

Although Al is the preferred element for oxidation resistance, the presence of a surface Cr_2O_3 scale results in significantly improved hot corrosion resistance. In general, the hot corrosion resistance is observed to scale with increasing Cr content (37). For this reason, the newer single crystal Ni-base superalloys, which typically contain lower amounts of Cr, exhibit decreased resistance to hot corrosion; whereas, the higher Cr content of the Co-base alloys results in significantly greater hot corrosion resistance. The other elements in most high temperature alloys have less obvious and consistent effects. For example, increased Al contents have been shown to result in increased oxidation resistance. However, Al_2O_3 does not exhibit long-term resistance to hot corrosion. Alloys with significant levels of Mo, W and V have been reported to exhibit reduced resistance to hot corrosion. However, additions of Ti and Ta resulted in increased resistance to hot corrosion.

5.3. Coatings. Since it is necessary for structural materials to exhibit environmental resistance, and the alloying to produce the needed environmental resistance often results in degraded mechanical properties, it has become quite common to apply coatings designed specifically for environmental resistance (38). The need for coatings only increases as the temperature increases and/or as the environmental resistance of the alloy decreases. Superalloy coatings typically provide a reservoir for aluminum and/or chromium for the growth of protective Al_2O_3 or Cr_2O_3 surface scales to reduce oxidation and corrosion damage. Pack cementation coatings can be relatively brittle high aluminum intermetallic phases, such as NiAl and CoAl, or can be relatively ductile lower aluminum alloy with a microstructure made up of the metal and the intermetallic (eg, Ni + NiAl). However, these diffusion coatings exhibit spallation during thermal cycling. Plasma spray MCrAlY coatings, where M is the metal matrix (ie, Ni, Co or Ni+Co), have been developed that exhibit a much greater resistance to thermal cycling. These overlay coatings utilize a high Al content for the formation of Al_2O_3 surface scale, but also rely on the fact that a reasonably high Cr content enhances the formation of the Al_2O_3 scale. The addition of Y, is that to impart an improved adherence of the oxide. Additions of Hf and Si have also been reported to produce enhanced adherence. It should be noted that the formation of the Al_2O_3 surface scale, results in the best resistance of oxidation. For the formation

of a spinel oxide with the base metal (ie, $NiAl_2O_4$) results in degraded environmental resistance. The spinels generally, exhibit faster growth rates and are less protective, and will degrade over time. The NiCrAlY coatings are known to exhibit superior elevated temperature oxidation, and the addition of Co to the coating results in improved hot corrosion resistance. The CoCrAlY coating is also known to exhibit excellent hot corrosion resistance.

Refractory metal alloys, which generally exhibit very poor resistance to oxidation, rely on silicide coatings, applied by pack cementation or slurry techniques (39). The silicide coatings generally include high levels of silicon combined with the refractory metal element. Generally, aluminide coatings have not been used as extensively as the silicides.

6. High Temperature Alloy Systems

6.1. Low Alloy Steels. The low alloy steels that can be used at elevated temperatures typically contain up to about 10 wt% Cr and up to about 1.5 wt% Mo, as well as small amounts of other elements. The relatively low alloy content of these alloys results in a reduced cost and, often times, reduced processing costs. Figure 17 clearly shows the creep properties of these types of steels.

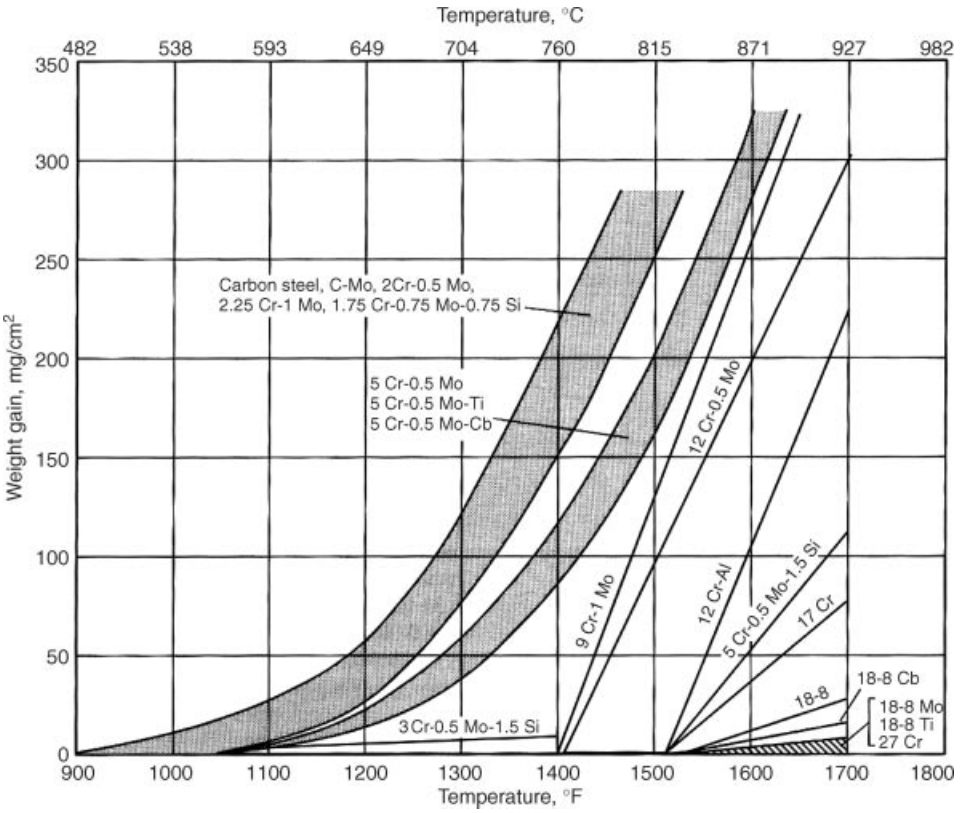

Fig. 17. Oxidation resistance of mild steels and low alloy steels in air after 1000hr exposures at elevated temperatures.

Table 2. **Compositions of Low Alloy Steels Typically Used for High Temperature Applications**

Alloy designation	Composition wt%, balance Fe							
	C	Mn	Si	P	S	Cr	Mo	other
C steel plate	0.17	0.90		0.035	0.045			0.25Cu
1Cr-0.5Mo	0.15	0.30–0.60	0.50	0.045	0.040	0.5–1.25	0.44–0.65	
1.25Cr-0.5Mo	0.20	0.50–0.80	0.60	0.04	0.045	1.00–1.50	0.45–0.65	
2.25Cr-1Mo	0.15	0.30–0.60	0.50	0.035	0.035	2.00–2.50	0.90–1.10	
9Cr-1Mo	0.20	0.35–0.65	1.00	0.04	0.045	8.0–10.0	0.90–1.20	

These alloys typically contain increased levels of Cr for oxidation and corrosion resistance (Table 2). Most of the low alloy steels contain between 0.5 wt% and 10 wt% and, in general, the oxidation/corrosion resistance scales with Cr content. The low alloy steels also contain increased levels of Mo for increased strength and increased pitting resistance. Mo is one of the most effective elements for increased creep resistance (Fig. 18). The low alloy steels typically contain between 0.5 wt% and 1.5 wt% Mo, which increases the creep strength of the

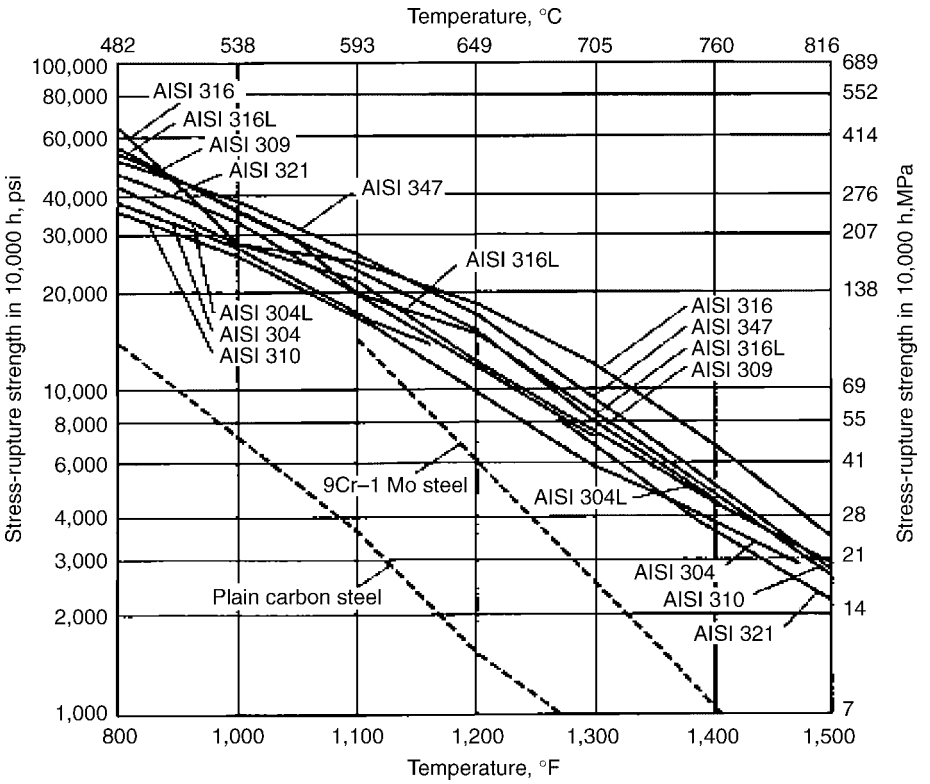

Fig. 18. Creep rupture strength of 300-series stainless steels. The creep strengths of plain carbon steel and 9Cr-1Mo steel are also shown for comparison.

alloys and also prevent temper embrittlement. The carbon contents of the low alloys steels are usually about 0.15 wt%, but higher levels can be seen in alloys intended for tooling and bolting applications. When improved oxidation resistance is needed, Si is often added. Higher temperature strengths can be obtained by increasing the stability of the carbides with the addition of vanadium or titanium. The addition of Ni is used when increased toughness is needed.

6.2. Wrought Stainless Steels. Stainless steels typically contain at least 12 wt% Cr and, generally, the oxidation/corrosion resistance increases with increasing Cr content. The wrought stainless steels are typically broken down into three distinct categories, as identified by the American Iron and Steel Institute (AISI). The 200-series alloys are austenitic due to the additions of Mn and nitrogen. Significant additions of Ni are used to stabilize the austenitic structure in the 300-series alloys. The 400-series alloys can be either ferritic or martensitic. The strengths of the alloys are presented in Figure 19.

The 200-series stainless steels are generally not used at elevated temperatures due to inadequate strength and oxidation resistance. The 300-series alloys

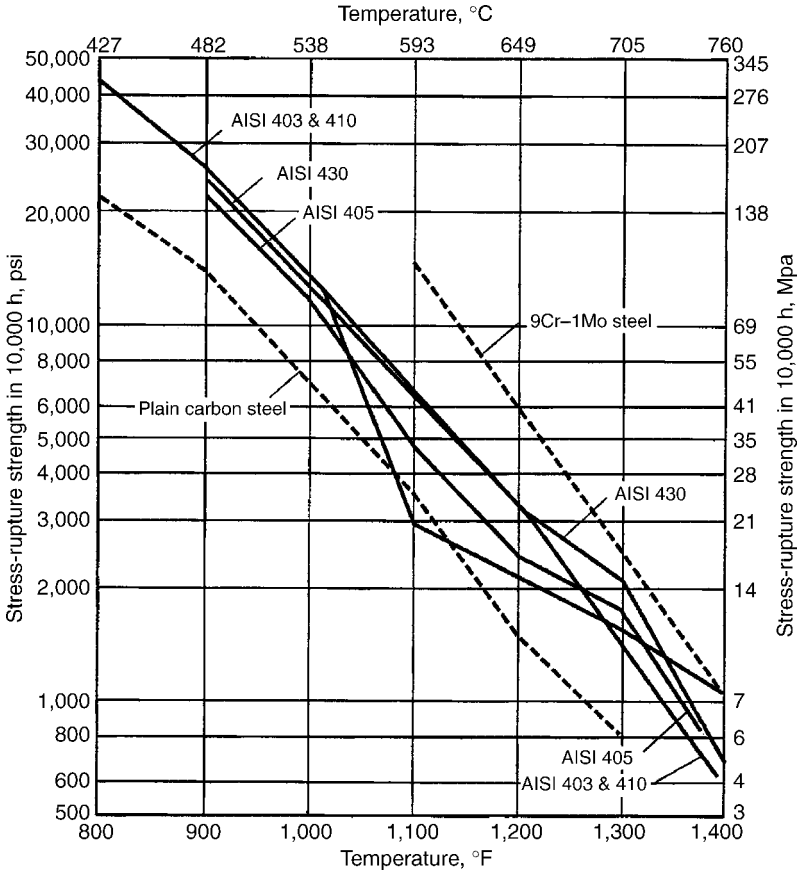

Fig. 19. 10,000h stress-rupture strength of 400-series stainless steels. The stress rupture strength of carbon steel and 9Cr-1Mo steels are also shown for comparison.

contain a minimum of 16 wt% Cr and 6 wt% Ni and can not be strengthened by heat treatment. For lower temperature applications, the 300-series alloys can readily be strain-hardened by cold work. But, for elevated temperature applications, the strain hardening is not an effective strengthening technique, as noted previously. The Mo-alloyed 316 stainless steel alloy is the highest strength 300-series alloy due to the solid solution strengthening by Mo. The 400-series alloys generally contain at least 11 wt% Cr, but only have at most another 2.5 wt% of other alloying additions. These 400-series alloys are either hardenable by the martensitic reaction or non hardenable (ferritic). The primary reason for this difference is the Cr content. These 400-series alloys have environmental resistance up to 1150°C, but exhibit only limited strength above about 600°C.

All of the stainless steels rely on the Cr_2O_3 surface scale for oxidation and corrosion resistance. As long as the Cr content of the alloy is above about 13 wt% Cr, the Cr_2O_3 is protective up to about 1000°C. However, if the intended application includes temperature cycling, the oxidation resistance of stainless steels may not be sufficient. Although the surface scale is protective for isothermal oxidation, the cyclic oxidation resistance is reduced to spallation of the oxide.

Although most of the stainless steels utilize wrought processing techniques, there are also cast versions of the alloys that are compositional very similar to the wrought varieties. The castings are classified as heat resistant when used at temperatures of 650°C or higher. The alloys are based on the Fe-Ni-Cr system, with the HC alloy equivalent to the AISI 446 and the HD alloy similar to the AISI 327 alloy. These alloys are generally used in metallurgical heat treatment furnaces, power generating plant equipment, gas turbines and glass manufacturing equipment. The alloys typically have 10–30wt% Cr for oxidation resistance and Ni contents up to 30 wt%. Alloys with higher Ni content generally exhibit increased strength, ductility and environmental resistance.

6.3. Modified Stainless Steels. Several modified versions of 12 wt% Cr, ferritic AISI 403 alloy have been developed. These alloys typically contain increased levels of Mo and/or tungsten to solid solution strengthen the matrix. All of the modified AISI 403 alloys are produced in a wrought form. Some of the alloys also utilize small additions of Nb and V for improvements in the primary carbide stability, while other alloys may also contain up to 2 wt% Ni, Cu and Al. All of these alloy modifications are intended to produce significant improvements in creep strength, without any reduction in environmental resistance. The modified versions of AISI 403 are typically used in the quench and temper condition and are often used for high temperature fasteners, turbocharger blades, boilers, superheaters and reheater tubes.

Some modified alloys are also precipitation hardenable by both a martensitic reaction and by precipitation hardening. These alloys also contain significant amounts of Cr for oxidation and corrosion resistance. Other alloying additions include Ni for reducing the kinetics of the martensitic reaction, Mo for solid solution strengthening and Nb for increased carbide stability. Some alloys also include Cu and Al for precipitation hardening. However, the temperature capabilities of the precipitation hardened alloys is less than that of the ferritic alloys.

6.4. Ni-Base Alloys. Ni-base alloys are, generally, used for corrosion and heat resistant applications, but can also be used for applications including coinage, battery electrodes, filters and catalysts (40–42). Nickel and Ni-base

alloys are vitally important to modern industry due to their ability to withstand a wide variety of severe operating conditions involving the combinations of corrosive environments, high temperatures and high stresses in one component or location (43,44). The reasons for this unique blend of properties stems from a variety of reasons, including the FCC crystal structure which exists in Ni-base alloys and ensures high ductility, and toughness. In addition, Ni-base alloys are readily fabricated by a variety of conventional processing techniques, including cast, wrought and powder metallurgy (P/M) methods.

Nickel has good resistance to corrosion in the normal atmosphere, in freshwater and in many acid and caustic environments. Since, Ni has excellent environmental resistance and is an excellent base on which to develop an alloy with unique properties or specialized applications.

Nickel has extensive solid solubility for many alloying additions, due to the partially filled 3d-orbital. The microstructure of Ni-base alloys consists of an austenitic or FCC solid solution, often called γ (gamma phase). Alloying additions can be added to form dispersoids and/or precipitates that can strengthen the alloy or increase the environmental resistance. Ni forms a complete solid solution with copper and has nearly complete solid solubility with iron. In addition, Ni can dissolve 35% chromium, 20% of molybdenum and tungsten, and between 5% and 10% of aluminum, titanium, manganese and vanadium. Therefore, the tough, ductile γ matrix can dissolve extensive amounts of alloying elements in various combinations that can provide solid solution strengthening, increase corrosion resistance and increase oxidation resistance. In general, the alloying additions with greater atomic size differences result in greater degrees of strengthening. Therefore, additions of tungsten, tantalum, niobium and molybdenum to the γ matrix result in significantly greater strengthening than iron and cobalt.

Additional strengthening can be obtained in Ni-base alloys by the precipitation of unique intermetallic phases between Ni and aluminum, titanium, niobium and tantalum. When the appropriate levels of these alloying elements are added to the Ni-base alloy, an age-hardening γ'-Ni_3(Al,Ti,Nb,Ta) or γ''-Ni_3(Nb,Ti,Al,Ta) precipitate is formed, depending on the composition of the resulting alloy. These precipitates result in alloys that exhibit very high strengths to significant fractions of the melting point of the Ni-base alloys. The combination or superposition of the solid solution hardening of the γ-matrix and the precipitation of the γ' or γ'' results in the alloys called superalloys, due to their unique balance of properties and high temperature capabilities.

Applications. Ni and Ni-base alloys are widely used in a wide variety of products for consumer, industrial, military, transportation, aerospace, marine and architectural applications. The unique balance of elevated temperature strength, corrosion resistance and fabricability make Ni and Ni-base alloys the material of choice for high-performance applications. For example, Ni-base alloys are widely used in chemical processing, power generation and aerospace propulsion industries when the need for high elevated temperature strength along with environmental resistance is difficult to meet.

Nickel-base superalloys are used for numerous applications, but none greater than in the gas turbine engine (45,46). The high temperature and high stresses encountered in gas turbine engines make superalloys the ideal material

for disks in the high pressure compressor and turbine sections, as well as for blades in these same locations within aircraft turbine engines. Superalloys for turbine applications are optimized for creep, tensile strength, crack growth rate and corrosion considerations in addition to other critical features.

Nickel and Ni-base alloys are used in a wide variety of application, although the majority of applications require a combination of strength, environmental resistance and/or heat resistance. Some of the more common applications include:

Aircraft gas turbines: disks, combustors, bolts, casing, shafts, exhaust systems, blades, vanes, afterburners, thrust reversers, etc.

Industrial/power generating gas turbines: disks, combustors, bolts, casing, shafts, exhaust systems, blades, vanes (buckets), etc.

Chemical processing industry: piping, bolts, fans, valves, flanges, reaction vessels, pumps.

Paper mills: tubing, blades, bleaching equipment, scrubbers.

Steam turbines: bolts, blades, tubing.

Metal processing: dies, tolling, fixtures.

Rocket engine: disks, blades, cases, combustors, bolts, shafts.

Heat treating equipment: furnace components, baskets, trays, fans, muffles.

Nuclear power systems: bolts, springs, valve stems, control rod drive mechanisms.

Reciprocating/automotive engines: turbocharger impellers, exhaust valves, glow plugs, catalytic converters.

Medical applications: prosthetic/implant devices, stints.

Corrosion Resistant Ni-base Alloys. Ni-base alloys can be processed by a powder metallurgy processing route and both casting and wrought ingot metallurgy processing techniques.

As noted above the corrosion resistant alloys are most commonly processed by wrought, ingot metallurgy techniques. However, casting and powder metallurgy techniques can also be used to produce unique corrosion resistant alloys or conventional alloys with unique shapes or properties. The majority of the corrosion resistant Ni-base alloys have compositions and processing to produce microstructures optimized for corrosion/oxidation resistance. In most cases, the environmental resistance is for aqueous corrosion resistance. However, more aggressive environments (eg, organic acids, alkalies, salts, seawater) and high temperature oxidation and sulfidation may also be encountered which require Ni-base alloys. In addition, many of the alloys developed for heat resistance, or elevated temperature service, may also exhibit excellent environmental resistance. Therefore, some overlap between environmental and heat resistant alloys may occur.

Since Ni has extensive solubility for a variety of alloying addition, many different commercial alloys have been developed and are readily available. As noted previously, Ni and Cu exhibit complete solubility, and Co and Fe exhibit very high levels of solubility with Ni. The limit of solubility for Cr is about 35–40%

and for Mo is about 20%. A lower limit for solubility for W in Ni is also observed. The γ-matrix in Ni-base alloys can be strengthened by solid solution strengthening, carbide precipitation or precipitation of an age-hardening phase (eg, γ' or γ''). Some alloys rely on only one of these strengthening mechanisms, while others utilize two or more of these methods to produce a corrosion resistant alloy with increased strength.

The solid solution strengthening in Ni-base alloys generally comes from the additions of Co, Fe, Cr, Mo, W, V, Ti and Al. However, the majority of solid solution strengthening comes from Mo and W. These elements all exhibit size differences, with respect to Ni, that can range from 1% to about 13%, with greater degrees of strengthening observed for greater lattice misfit (47). It should also be noted that the strengthening resulting from solid solution alloys is effective at all temperatures up to the melting point of the alloy. Therefore, the solid solution strengthened alloys can be used for elevated temperatures service (ie, >0.5 T_m, where T_m is the melting temperature or solidus of the alloy). At the highest temperatures, Mo and W are the most effective solid solution strengtheners and also result in reduced diffusion rates which further increases the creep strength of the alloy. However, care must be taken to avoid adding excessive levels of elements such as Cr, Mo and W since these elements can result in microstructural instabilities that can be detrimental for mechanical properties (eg, toughness, ductility, creep strength and fatigue resistance).

Most Ni-base alloys also contain both primary and secondary carbides. Since Ni is not a carbide former, carbon reacts with other elements within the Ni-base alloy, such as Ti, Nb, Ta, and Cr. The presence of these carbides can result in both improved creep strength and corrosion resistance, but may result in reduce fracture toughness and ductility. The primary, MC-carbides, where M denotes a metallic element, such as Ti, Nb or Ta, form during solidification and are usually relatively coarse in size and exhibit a blocky morphology. These MC carbides generally do not have a significant impact on mechanical properties, although they can act as crack initiation sites in cyclic or fatigue testing. Instead the MC carbides generally act as a reservoir for the formation of secondary carbides and aid in the control of the γ matrix grain size. The most common secondary carbides have compositions of $M_{23}C_6$ and M_6C, where M denotes the metallic elements, such as, Cr, Mo, and W, and are found at grain boundaries. $M_{23}C_6$ carbides typically comprised to a large extent Cr. M_6C is known to form in alloys with percentage of Mo + W greater than 6%. Although the MC carbides form during solidification, the secondary carbides form during subsequent heat treatment and generally improve the strength of grain boundaries. In particular, the secondary carbides are known to increase the creep strength of an alloy by strengthening the grain boundary and preventing or limiting grain boundary sliding. In addition, the secondary carbides are also reported to increase the stress corrosion cracking (SCC) resistance of Ni-base alloys.

The precipitation of γ'-Ni_3(Al,Ti) and γ''-Ni_3(Ti,Nb,Al) in Ni-base alloys results in alloys with significant strength levels at all temperatures (48,49). γ'' forms in alloys with relatively large amounts of Nb compared to Ti and Al, such as Alloy 718 and Alloy 706. The γ'' precipitate results in significant strengthening due to large lattice mismatch with the γ matrix resulting in high degrees of coherency strengthening. However, the strengthening due to

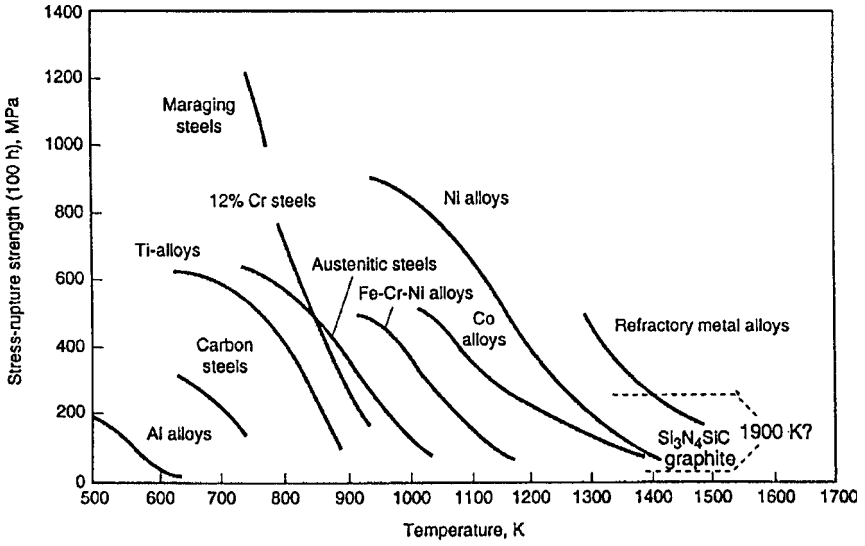

Fig. 20. Maximum service temperature, based on 100hr stress rupture strength, for various creep resistant materials.

the precipitation of γ'' is only useful at temperatures below approximately 700°C. The high level of lattice mismatch results in instability and coarsening of the γ'' precipitate at elevated temperatures, which results in reduce strength.

The alloys with γ/γ' microstructures are generally referred to as the superalloys (Fig. 20) and can be used temperatures approaching $0.9T_m$, where T_m is the absolute melting temperature or solidus in an alloy (48, 50). Varying degrees of lattice mismatch are observed between the γ matrix and γ' precipitates depending on alloy chemstry. Therefore, the γ' precipitates can be engineered to be stable to much higher temperatures with alloy chemistry combinations that provide relatively low mismatch. γ' can be dissolved and precipitated in controlled manners for optimum particle size and distribution. Many heat treatment schemes are based on this capability, with solution temperatures set relative to each respective alloy's γ' solvus temperature. The superalloys typically have between 20 and 70 volume % of γ', with higher strengths being observed in alloys with higher volume fractions of γ'. However, alloys with increased γ' volume fractions typically also exhibit increased difficulty in fabrication and joining.

Boride phases are also formed in numerous nickel-base superalloys. These secondary phases (M_3B_2 and MB_2) precipitate upon cooling from high temperature, similar to the manner of secondary carbides. Boride phases act similar to carbides to increase grain boundary properties and increase overall elevated temperature capabilities.

7. Commercial Nickel and Ni-base Alloys

An incomplete list of commonly used Ni-base alloys and their properties are presented in Tables 3–6.

Table 3. **Compositions (in wt%) of Common Ni-base Alloys**[a]

ALLOY	Cr	Ni	Co	Mo	W	Nb	Ti	Al	Fe	C	B	Other
Ni 201		bal								0.02		
Ni 211		bal								0.20		4.75 Mn
Duranickel		bal					0.65	4.5		0.3		1.0 Si
Alloy 360		bal					0.5					2.0 Be
Monel 400		bal							2.5	0.3		31.0 Cu
Monel 401		bal							0.75	0.1		2.25 Mn, 65 Cu
K-500		bal					0.65	2.75	2.0	0.25		1.5 Mn
Hastelloy B	1.0	bal	2.5	29.5					6.0	0.12		
Inconel 600	15.5	bal							8.0	0.15		
Inconel 601	23.0	bal						1.35	15.0	0.10		
Inconel 690	29.0	bal							9.0	0.05		
Haynes 214	16.0	bal	2.0				0.5	4.5	3.0	0.05		
Incoloy 800	21.5	33.5					0.4	0.4	bal	0.10		1.5 Mn
Incoloy 825	21.5	42.0		3.0			0.9	0.2	bal	0.10		1.0 Mn
Hastelloy C	15.5	bal	2.5	16.0	3.75				5.5	0.08		0.35 V
Inconel 625	21.5	bal		9.0		3.6	0.2	0.2		0.05		
Inconel 617	22.0	bal	12.5	9.0			0.6	1.2	3.0	0.10	0.006	0.5 Cu
Hastelloy S	21.0	bal		15.3	3.7		0.2		3.0	0.02	0.015	0.35 Cu
Haynes 230	22.0	bal		2.0	14.0			0.35	3.0	0.10	0.015	0.7 Mn, 0.010 La
Inconel 718	19.0	52.5	1.0	3.1		5.2	0.35	0.7	bal	0.08	0.06	
Inconel 725	21.5	57.0		8.2		3.2	1.4	0.35	bal	0.03		
625 Plus	21.5	60		8		3.2	1.4	0.35	bal	0.03		
625M	21.5	bal		9.0		5.2	0.35	0.7		0.03		
Invar		36							bal			
Elinvar	4.5	34			2.0				bal	1.2		1.2 Mn, 1.2 Si
Incoloy 909		38	14.0			4.9	1.6	0.15	bal	0.06	0.012	0.4 Si

[a]Refs. 40–42.

Table 4. **Typical Room Temperature Tensile Properties, for Select Ni-base Alloys**[a]

Alloy	Yield strength, MPa	Ultimate tensile strength, MPa	Elongation, %	Young's modulus, GPa
Nickel 200	150	450	45	204
Nickel 201	100	400	50	207
Nickel 211	240	530	40	207
Duranickel 301	860	1150	25	207
Monel 400	250	550	40	180
Monel 401	135	450	50	180
K-500	800	1100	20	180
Inconel 600	300	650	40	207
Inconel 601	275	600	45	207
Inconel 617	350	750	50	207
Inconel 625	500	900	40	207
Inconel 690	350	725	40	207
Inconel 718	1000	1250	15	207
Incoloy 800	300	600	45	193
Incoloy 825	300	700	45	207

[a]Refs. 40,41.

7.1. Commercially Pure Ni Grades. Commercial purity Ni grades, such a Nickel 201, typically have minimum Ni contents of 99% and are highly resistant to many corrosive and oxidizing environments. Tight control on impurities and intentional additions is used to maintain the high purity levels. In most alloys carbon levels of 0.1–0.15 wt% are observed, which can limit the maximum use temperatures to about 315°C, due to the potential for embrittlement of the alloy. In general, commercial purity alloys exhibit moderate strengths, good ductility and high toughness and are typically used for chemical processing and the electronic industry. Annealed yield strengths of 100–150 MPa and elongations of 40–50% are commonly observed. Cold worked materials have been reported to exhibit strengths in excess of 600 MPa and ductilities of less than 10%. These

Table 5. **Typical Room and Elevated Temperature Properties of Selected Cast and Wrought Ni-base Superalloys**[a]

	Room temperature			540°C			870°C		
Alloy	YS	UTS	Elongation, %	YS	UTS	Elongation, %	YS	UTS	Elongation, %
CMSX-4	1150	1225	10	1275	1325	17	850	1100	20
IN 100	850	1015	9	875	1100	7	700	885	6
IN 738	895	1095	7	900	1090	7	550	770	11
MarM 247	815	965	7	825	1035	7	690	825	7
Nimonic 80A	620	1000	39	530	875	37	260	310	30
PWA 1480	895	1100	4	900	1130	8	705	995	12
Udimet 700	965	1400	17	1170	1275	16	635	690	27
Waspaloy	800	1275	23	725	1170	23	250	275	35

[a]Refs. 40,41,51.

Table 6. **Typical Elevated Temperature 100- and 1000-hour Stress Rupture Strengths for Selected Cast and Wrought Ni-Base Superalloys**[a]

	815°C		870°C		980°C	
Alloy	100 h	1000 h	100 h	1000 h	100 h	1000 h
CMSX-4	800	600	625	450	290	200
IN 100	455	365	360	265	140	90
IN 738	430	315	295	215	130	90
MarM 247	585	415	455	290	195	125
Nimonic 80A	195	85	97		15	
PWA 1480	600	450	475	335	210	145
Udimet 700	400	325	295	200	110	55
Waspaloy	275	200	175	110	45	

[a]Refs. 40,41,51.

alloys are readily fabricated and welded in a variety of applications and are most frequently processed by wrought (ingot) metallurgy techniques.

7.2. Low-Alloy Nickel Alloys. Alloys which have a minimum Ni content of 94% are considered low-alloy Ni alloys. Additions of up to 5 wt% Mn (Nickel 211) or up to 5 wt% Al and 0.6 wt% Ti (Duranickel) are used to increase the resistance of the alloy to sulfur embrittlement and corrosion/oxidation, respectively. It should also be noted, though, that the high Al + Ti content of Duranickel will result in the precipitation of γ', which will produce significant strengthening. In some alloys (alloy 360), additions of up to about 2 wt% Be and 0.5 wt% Ti are used for increased strength due to a precipitation hardening reaction. The precipitation hardened alloys, including both Duranickel and alloy 360 exhibit significantly higher strengths and lower ductilities than the commercially pure Ni alloys and the low-alloy Ni alloy, Nickel 211. In most cases, the low-alloy Ni alloys are processed by wrought (I/M) processing techniques, but the Ni-Be alloys (alloy 360) can be processed by both cast and wrought ingot metallurgy techniques. Joining of the low-alloy Ni alloys can be more difficult for the precipitation hardened alloys due to the potential for of strain age cracking.

7.3. Nickel-Copper Alloys. Most Ni-Cu alloys (Monel 400) contain approximately 25–40 wt% Cu for solid solution strengthening and were developed for corrosion resistant applications. Some Ni-Cu alloys have higher Cu contents (Monel 401) and some alloys (K-500) contain additions of Al and Ti for precipitation hardening from γ'. Most Ni-Cu alloys exhibit moderate strength, high ductility, and high toughness. However, the precipitation hardened alloys can exhibit much higher strengths, but reduced ductility and toughness. In general, the Ni–Cu alloys exhibit good resistance to corrosion and stress corrosion cracking in a variety of environments. Most Ni–Cu alloys are processed by wrought (I/M) processing techniques, but some alloys can be processed by casting. The fabricability and joining of the Ni–Cu alloys is generally quite good, however, strain age cracking can occur in the age-hardenable alloys (K-500). The Ni–Cu alloys can be used in the annealed condition or after cold work to increase the strength of the material.

7.4. Nickel-Molybdenum Alloys. Approximately 25–30 wt% of Mo is added to Ni-Mo alloys to confer resistance to acid and other reducing environments. The Ni-Mo alloys (Hastelloy B) exhibits excellent resistance to boiling hydrochloric acid and is widely used in the chemical processing industry. Other alloys have been developed with reduced levels of impurities which exhibit even greater resistance to severe environments. However, these alloys exhibit very poor elevated temperature oxidation resistance due to the lack of elements such as Cr and Al. In addition, some of the Ni-Mo alloys can exhibit reduced mechanical properties due to microstructural stability concerns following long-term elevated temperature exposures. The vast majority of Ni-Mo alloys are processed by wrought (I/M) processing techniques and can be readily joined using standard techniques.

7.5. Nickel-Chromium-Iron Alloys. The addition of 15–30 wt% Cr to Ni-Cr-Fe alloys results in the formation of a very protective Cr_2O_3 surface oxide that resistance both corrosion and oxidation to high temperatures. The Ni-Cr-Fe alloys (Alloys 600 and 690) exhibit moderate strength to elevated temperature, excellent corrosion resistance in a variety of environments, immunity to stress corrosion cracking, and resistance to hot corrosion. Several of the alloys can be used to temperatures approaching 1200°C for long-term applications. Most Ni-Cr-Fe alloys are single phase austenitic materials with both primary and secondary carbides and can be readily fabricated into a variety of forms, most commonly through wrought (I/M) processing techniques. However, some applications an utilize casting and powder metallurgy processing. Some alloys which are considered Ni-Cr-Fe alloys also contain additions of Al (Alloys 601 and 214) for improved oxidation resistance at the highest temperatures, but may be more difficult to weld and fabricate and may have limited thermal stability due to the formation of γ'. The Ni-Cr-Fe alloys are widely used for elevated temperature service from gas turbines, steam generators, mechanical property testing equipment, chemical processing and nuclear reactors.

7.6. Iron–Nickel–Chromium Alloys. The Fe-Ni-Cr alloys are similar to the Ni-Cr-Fe alloys, but have increased Fe contents for reduced cost (51). These alloys are also similar to austenitic stainless steels, but have significantly higher Ni contents. The Fe-Ni-Cr alloys (Alloy 800) exhibit good oxidation/corrosion resistance, stress corrosion resistance and moderate strength to moderate temperatures. These alloys are very fabricable and weldable and are most commonly fabricated by wrought (I/M) processing techniques. The Fe-Ni-Cr alloys are used extensively for chemical processing and power generation. Higher strength Fe-Ni-Cr alloys can be produced by the addition of Mo for solid solution strengthening and the addition of Al and/or Ti for γ' precipitation (Alloy 825). The Mo addition will also increase the pitting corrosion resistance of the alloy. However, the fabricability and weldability of these higher strength Fe-Ni-Cr alloys will be reduced.

7.7. Nickel–Chromium–Molybdenum(Tungsten) Alloys. A large number of Ni-Cr-Mo(W) alloys have been developed and are widely used in gas turbines, nuclear applications, chemical processing, pollution control and waste treatment. These alloys typically have 15–30 wt% Cr and 5–20 wt% Mo and/or W, but other additions of Fe, Co, Al and Ti are also common. The Ni-Cr-Mo(W) alloys typically are processed by wrought (I/M) processing techniques and can be

fabricated in a variety of forms and can be readily joined. Alloys such as the Hastelloy C series and Alloy 625 are widely used in chemical processing, due to their excellent resistance to general corrosion and pitting corrosion. However, care must be taken during welding to prevent the sensitization of the structure to stress corrosion cracking. Most of the alloys, including Alloys 617 and 625, and Hastelloy S, have compositions that have been balanced to produce a stable microstructure. In particular, the levels of Fe, Mo and W are controlled to prevent the precipitation of deleterious phases. Higher strength can be obtained in these alloys by solid solution strengthening by increased levels of Mo and W (Alloy 230) and Co (Alloy 617). Additional oxidation resistance can be imparted by the additions of Si, La and Mn. Generally, higher Fe contents result in reduced creep strength and oxidation resistance. In most applications, these alloys are used in relatively low stress applications that require oxidation/corrosion resistance, weldability and fabricability (eg, combustor cans in a gas turbine, heat treatment racks and piping for chemical processing).

7.8. Precipitation Hardened Ni-base and Ni-Fe-base Alloys. The need for high strength, corrosion resistant alloys for fastener and drilling equipment applications in sour gas wells led to the development of precipitation hardened Ni-base and Ni-Fe-base alloys. These alloys are related to alloys 625 and 718 and utilize γ''-Ni_3(Nb,Ti,Al) for increased strength. The alloys (Alloy 725, 625 Plus and 625M) typically utilize high Cr and Mo contents for corrosion and stress corrosion cracking resistance (from alloy 625) and elevated levels of Nb, Ti and Al for precipitation of γ'' (typical of alloy 718). These alloys are most frequently processed using wrought (I/M) techniques, but alloy 625M was developed for powder metallurgy (P/M) processing. The maximum strength of these alloys relies on some of the residual work from wrought processing. Welding of these materials is possible, since alloys strengthened by γ'' precipitation are less likely to exhibit strain age cracking (Figs. 21 and 22). However, the strength, and possibly, the corrosion resistance, of the weld region will not be equivalent to the base metal.

7.9. Controlled Expansion Alloys. The coefficient of thermal expansion of most structural alloys range are the range of $5–25 \times 10^{-6}$m/m·K. However, for some applications, a reduced coefficient of thermal expansion would be beneficial to reduce stresses due to heating and cooling, to control tolerances between components, and match the thermal expansion of dissimilar materials (eg, joining metals to ceramics). Typical applications of controlled expansion alloys include pendulums and balance wheels for clocks and watches, glass-to-metal joints, vessels and piping for cyrogenic liquids, superconducting systems in power transmission, integrated circuit lead frames, components for radios and other electronic devices and structural components in precision measurement systems. Most controlled expansion alloys are made-up of nickel, cobalt and iron with small additions of C, Si, Cu, Cr and Mn.

The controlled expansion alloys contain Ni addition to Fe since Ni has a profound effect on the thermal expansion of Fe. Depending on composition, Ni-Fe alloys exhibit thermal expansions that range from -0.5×10^{-6}m/m·K to 20×10^{-6}m/m·K. Generally, most controlled expansion alloys contain 30–60 wt% Ni, since virtually any expansion characteristic can be selected from the alloys within this range. The alloys generally contain a total of 1 wt% or less of Mn, Si and C. Invar (Fe-36 wt%Ni) is one of the most common controlled

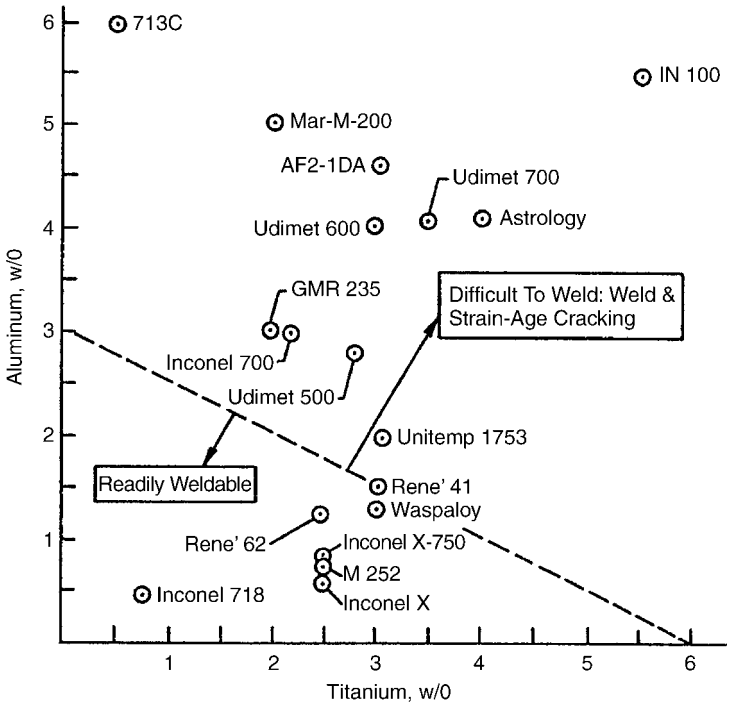

Fig. 21. Weldability of Ni-base alloys, as a function of Al and Ti content. Increased Al and Ti contents will result in larger amounts of γ', which forms relatively quickly during cooling. Increased volume fractions of γ' will result in reduced weldability.

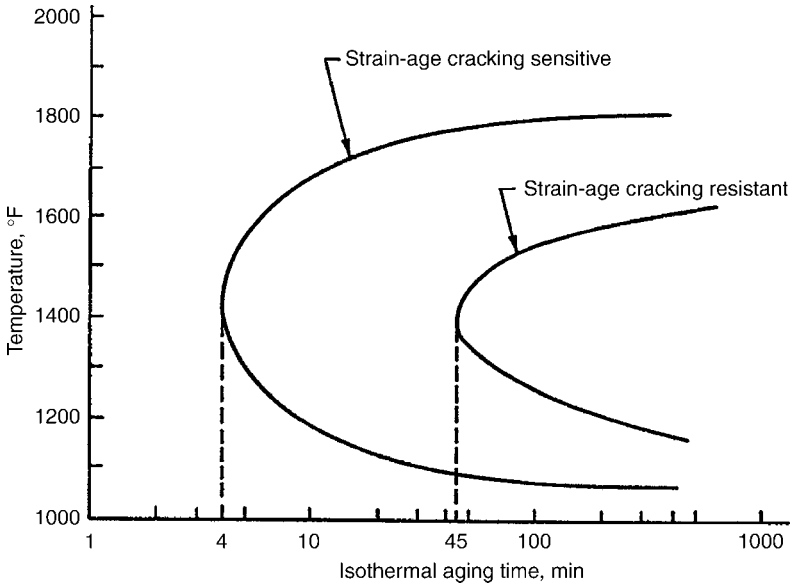

Fig. 22. Isothermal, time-temperature transformation curves for the indication of cracking due to strain age cracking in alloy Rene' 41. The strain-age cracking resistant materials generally form lower volume fractions of γ' and form the γ' at a slower rate.

expansion alloys used in industry and is the Fe-Ni composition which exhibits the minimum in coefficient of thermal expansion. The maximum temperature for minimum thermal expansion is about 275°C, but, it should also be noted, that these Fe-Ni alloys would be expected to exhibit poor oxidation/corrosion resistance at high temperatures. The addition of third and fourth elements to the Fe-36 wt% Ni alloys for improved properties will have a significant impact on the thermal expansion characteristics. In addition, processing and heat treatment has a significant impact on the thermal expansion coefficient. Most of the controlled expansion alloys are processed by wrought (I/M) techniques and great care must be taken to obtain reproducible properties.

Small additions of 2–8 wt% Cr to produce Fe-Ni-Cr alloys (Elinvar) with controlled expansion result in an alloy with a limited amount of oxidation/corrosion resistance (40, 41). Further reduction in the thermal expansion coefficient can be achieved by the substitution of a limited amount of Co (about 5 wt%) for Ni, producing Fe-Ni-Co alloys, such as Kovar. These alloys are used for making glass-to-metal seals, but exhibit poor oxidation/corrosion resistance.

High strength, controlled expansion alloys have been developed that contain Nb, Ti and Al additions to form γ''. These alloys are based on the Fe-Ni-Co system and are useful to temperature approaching 500°C. These alloys (alloy 909) have been used for applications for improved tolerances, which result in improved efficiencies in gas turbines and rocket engines. Unlike the other controlled thermal expansion alloys, the high strength alloys can be processed by both wrought and cast (I/M) techniques. However, care must be taken in weld repair of large casting due to the potential for strain age cracking.

7.10. Precipitation Hardened Ni-base Superalloys. The superalloys are generally high strength, corrosion resistant Ni-base alloys that are used at temperatures in excess of about 540°C. However, there are many subcategories within the field of precipitation hardened Ni-base superalloys which will be discussed below. There are two major types of precipitation hardened Ni-base superalloys. The first type achieves high strengths due to the precipitation of γ'' (alloys 718 and 706) and can be used up to temperatures approaching 750°C. Significantly higher temperature capabilities are observed in the γ' strengthened superalloys (Mar-M247, IN738, Udimet 720 and CMSX-4). The γ' strengthened superalloys typically contain 20–70% volume fractions of the precipitate and can be used up to temperatures approaching 90% of the melting temperature (ie, 1100–1200°C). The primary application for the superalloys include industrial, power generating and aerospace propulsion gas turbines. Other applications of the superalloys include nuclear reactors, aircraft structures, spacecraft structures, petrochemical processing, orthopedic and dental prosthesis. Superalloys have been used in cast, wrought and powder processed forms. Each processing wrought has unique requirements and often unique alloy compositions and will be discussed separately below.

Both types of precipitation hardened Ni-base superalloys typically contain additions of Co, Cr, Mo, W, Re, Al, Ti, Ta, Nb, V, C, B, Zr, and Hf. Other elemental additions are also utilized for specialized applications. The addition of Co results in increased workability in wrought alloys and improved heat treatment response in high volume fraction cast alloys. Cr additions are typically made for

increased oxidation and hot corrosion resistance. However, elevated levels of Cr can result in reduce high temperature strength and reduced microstructural stability. Solid solution strengthening of the γ matrix phase is accomplished with additions of Mo, W, and, in a few cases, V. In high strength single crystal cast superalloys, additional solid solution strengthening is achieved with the addition of Re. The addition of Al, Ti, Nb and Ta result in the formation of the precipitation for increased strength. The γ' hardened alloys typically rely on high levels of Al, with moderate levels of Ti, Nb and Ta. Excessively high levels of Ti, Nb and Ta can detrimentally effect the stability of the γ'. The γ'' is formed in alloys with elevated levels of Nb and Ti, and moderate levels of Al. Ta additions are not frequently used in γ'' strengthened alloys. In some γ'' strengthened alloys, both γ' and γ'' are observed and, in some cases, the γ' is reported to be the nucleation site for the γ'' precipitation. It should be noted that γ' quickly precipitates from the supersaturated γ matrix during cooling from elevated temperatures or during aging heat treatments. However, the nucleation kinetics for the formation of γ'' are significantly slow and rely on either specific elements (eg, Ti) to act as a catalyst, or another phase (eg, γ') or deformation to act as a nucleation site. The more sluggish formation of γ'' is one of the reasons that γ'' strengthened alloys are much more readily welded than γ' strengthened alloys.

The grain boundaries of polycrystalline alloys are strengthened by the addition of C, B, Zr and Hf. The presence of secondary carbides at the grain boundaries prevents grain boundary sliding during creep deformation (40–42,48,50). In addition, B, Hf and Zr are believed to increase the strength of the boundaries during elevated temperature service and processing. However, all of the grain boundary elements significantly reduce the solidus temperature of Ni-base superalloys. In some alloys, complete solution the γ' during heat treatments is not possible due to the suppression of the solidus below the γ'-solvus temperature by the addition of C, B, Zr, and Hf. Single crystal, alloys which do not contain high angle grain boundaries, utilize much lower levels of these grain boundary elements, and in some cases, totally eliminate these elements from the alloys. Most of the single crystal alloys, therefore, can be heat treated to allow complete dissolution and reprecipitation of the γ' in a controlled fashion to maximum the effectiveness of the precipitation hardening. Low levels of these grain boundary elements are frequently observed to provide increased castability, defect tolerance and oxidation/hot corrosion resistance.

As noted above the alloy compositions of the Ni-base superalloys are tailored not just for processing, but also for the application. For example, alloys traditionally intended for industrial gas turbine applications must be resistant to hot corrosion, and, therefore, have high Cr (eg, 10–18 wt%) contents and increased Ti/Al-ratios. Aircraft engine alloys require greater levels of oxidation resistance and will have higher Al contents (lower Ti/Al-ratios) and lower Cr contents (2–12 wt%). In addition, the aircraft engine alloys are typically utilized at higher temperatures and increased creep strength is required. In order to achieve the higher strength, aircraft engine alloys typically have higher Ta contents (increase γ' volume fraction and strengthening of γ') and increased levels of refractory metal additions (W, Mo, Re) for solid solution strengthening. However, many of these alloy modification for increased strength decreased fabricability and castability.

Wrought alloys typically have somewhat lower volume fractions of γ' (20–50 vol %) and lower C contents than cast alloys. The reduced γ' volume fractions and carbon levels are necessary to increase the hot workability of the alloy. Wrought alloys also typically have elevated levels of Co (workability) and Cr (environmental resistance) than many cast alloys. Cast alloys will have elevated levels of all of the γ' formers (Al, Ti, Ta, Nb) and carbon, for increased elevated temperature strength (Figs. 23, 24 as example). Directionally solidified alloys to produce columnar-grained materials will have elevated levels of Hf (1.0–1.5 wt%) to prevent cracking during casting. As noted above, the single crystal

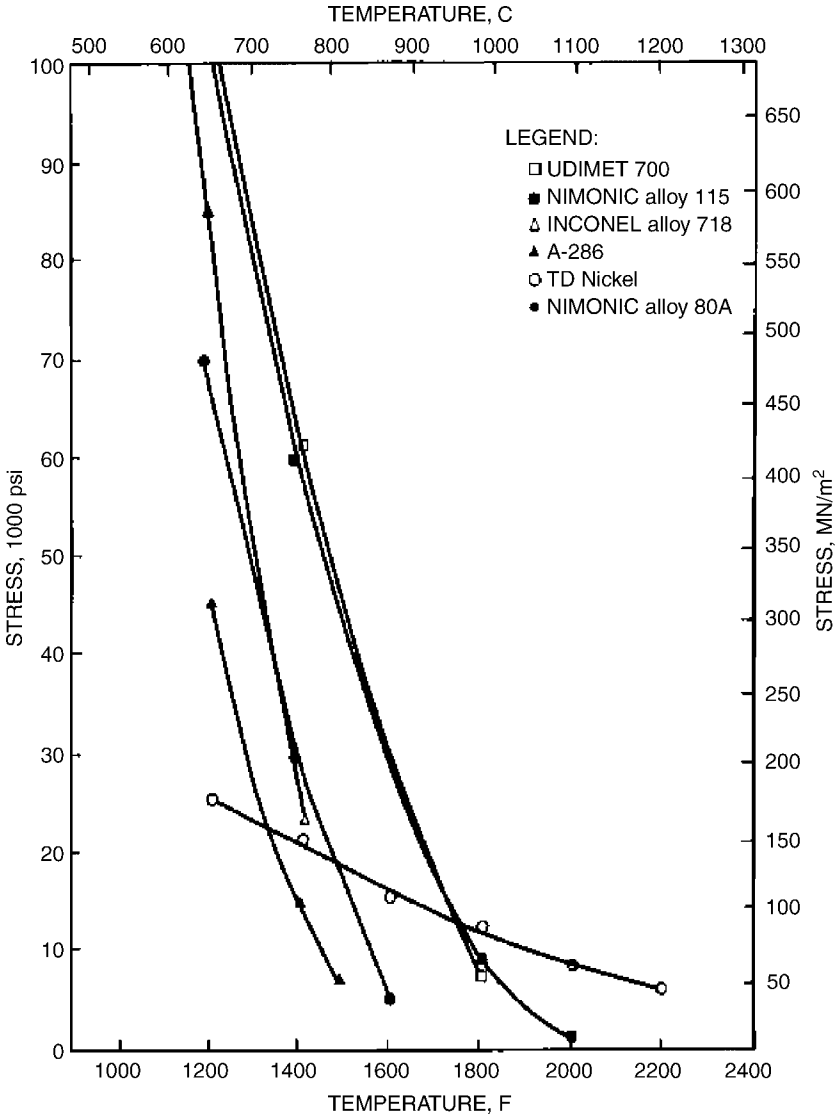

Fig. 23. 1000- hr stress rupture properties of select wrought Ni-base superalloys.

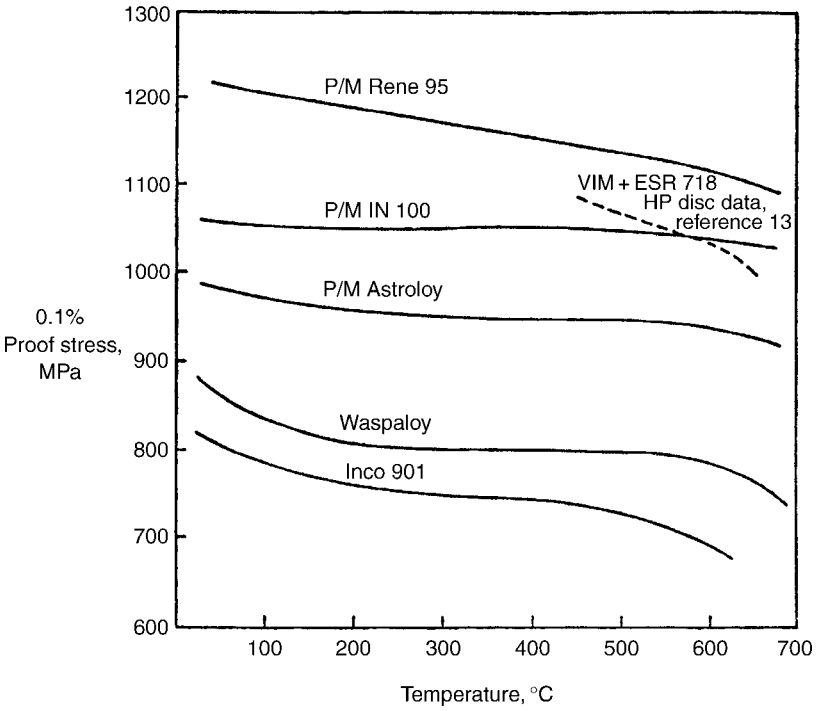

Fig. 24. Effect of temperature on the 0.1% proof stress of selected powder metallurgy (P/M) and wrought superalloys.

alloys contain much lower levels of the grain boundary strengtheners and even higher levels of the γ' formers (Al, Ta, Ti, Nb) and solid solution strengtheners (W, Mo, Re, Ru) and decreased levels of Cr. Powder metallurgy alloys are similar to wrought alloys, in that they have reduced levels of the grain boundary elements and increased Cr and Co levels. However, the powder metallurgy alloys also contain higher levels of γ' formers (Al, Ti, Nb, Ta). The powder metallurgy alloys typically have higher γ' volume fractions than the wrought alloys and could not be easily processed by conventional ingot metallurgy techniques. The higher γ' volume fractions and, in some cases, higher solid solution strengthener levels, would be difficult to cast, without excessive segregation and cracks, and deformation process. Powder metallurgy processing is often the only viable processing method for these alloys (Rene' 95, IN100, AF2-1DA).

8. Other Commercial Alloys

8.1. Co-Base Superalloys. Co-base superalloys are principally used in highly corrosive environments at temperatures ranging from 650–1000°C and usually at low stress levels (Table 7 and Fig. 25). These alloys are frequently used in industrial gas turbine blades/vanes and as combustor liners and afterburner components (52). These alloys are produced in both wrought and cast

Table 7. **Composition of Co-base Superalloys**

Alloy designation	Cast or wrought	Composition (wt%), balance Co								
		Ni	Cr	W	Ta	Nb	Ti	C	Zr	Other
Haynes 188	wrought	22.0	22.0	14.0				0.10		1.5 Fe, 0.75 Mn, 0.40 Si, 0.08 La
L-605	wrought	10.0	20.0	15.0				0.10		1.50 Mn, 0.50 Si
FSX-414	cast	10.0	29.0	7.5				0.25		1.0Fe, 0.01 B
MarM-302	cast		21.5	10.0	9.0			0.85	0.20	0.005 B
MarM-509	cast	10.0	23.5	7.0	3.5		0.20	0.60	0.50	
WI-52	cast		21.0	11.0		2.0		0.45		2.0 Fe, 0.25 Mn, 0.25 Si
X-45	cast	10.5	25.5	7.5				0.25		0.75 Si

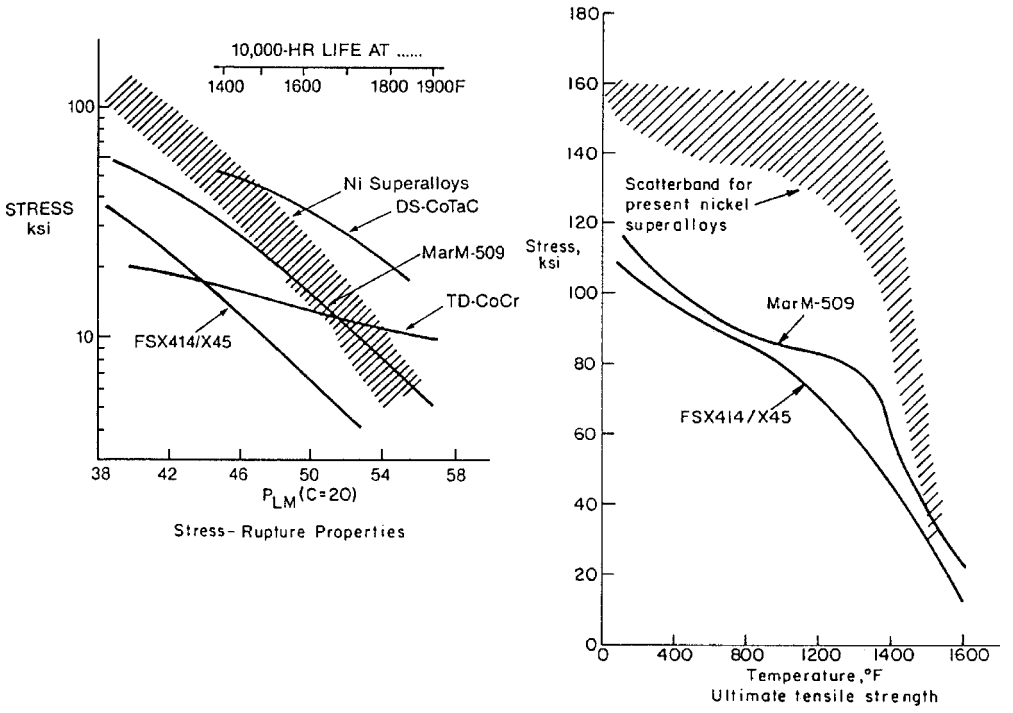

Fig. 25. Comparison of the stress rupture properties and ultimate tensile stress of Co-base alloys (FSX-414/X-45, MarM-509) and Ni-base alloys. Several experimental Co-base alloys (eg, TD-CoCr and DS-CoTaC) are also included in the stress rupture properties.

forms and are strengthened by both solid solution and carbide precipitation. Since the chemistries of the Co-base superalloys is simpler than the more highly alloyed Ni-base superalloys, the thermal conductivity of Co-base alloys is significantly greater than Ni-base alloys. Therefore, Co-base alloys are more resistant to thermal fatigue and thermal shock than Ni-base alloys. In addition, the Co-base alloys typically have significantly higher Cr contents and will exhibit greater hot corrosion resistance than Ni-base alloys (53). Therefore, Co-base alloys are more likely to be used as stationary components in a gas turbine, but the Ni-base alloys are more likely to be used for rotating components due to their higher strengths at low and intermediate temperatures.

Co-base alloys typically have Cr contents in the range of 20–35 wt% and carbon contents can exceed 1 wt% in cast alloys (54). The carbon content of wrought alloys is significantly lower and is usually in the range of 0.1 to 0.5 wt%. This high carbon level results in a large volume fraction of carbides that form on stacking faults throughout the material. These carbides dispersion harden the alloy to very high temperatures. However, as noted previously, dispersion hardening is not as effective as the coherent γ' precipitates in the Ni-base superalloys. The high temperature stability of the carbides in Co-base superalloys results in a significant amount of dispersion hardening at very high temperatures. In fact, since the Co-base alloys utilize both solid solution and dispersion strengthening, both of which are useful to very high temperatures, many Co-base alloys are useful to temperatures exceeding 1100°C. No intermetallic compound, like γ' in Ni-base alloys, has been identified in Co-base alloys, which limits the amount of low and intermediate temperature strength in Co-base alloys.

Many of the early Co-base alloys do not require vacuum processing, which results in considerable cost savings. The newer alloys, however, contain more volatile elements, such as Ta, Ti and Y, which requires the use of vacuum melting.

In general, the Co-base superalloys rely on the high levels of Cr in the alloy to form protective Cr_2O_3 surface scales for oxidation resistance. In some alloys the protectiveness and stability of the Cr_2O_3 is enhanced (55) by the addition of rare earth elements (eg, Y, Ce, La). The Cr_2O_3 is also provides excellent hot corrosion resistance for the Co-base superalloys. In some cases, the alloys can be coated with a CoCrAlY-type coating for further improvements in environmental resistance.

8.2. Refractory Metals and Their Alloys. The refractory metal elements (ie, Mo, W, Cr, Ta, Nb and V) are of obvious interest for high temperature applications due to their melting points (Table 8 and Fig. 26). V and Cr melt at temperatures just below 2000°C, Mo and Nb melt at temperatures above 2700°C and W and Ta melt at temperatures about 3000°C. However, these body centered cubic (BCC) metals are not always considered for high temperature applications due to their poor oxidation resistance, with the exception of Cr. In addition, several of the alloys exhibit limited ductility, and Cr, in particular, exhibits very limited ductility and low room temperature toughness. Mo and W also exhibit limited ductility and low temperatures, but some increases in ductility can be achieved with alloying and thermo-mechanical processing. Nb, Ta and V all exhibit relatively high ductility levels, but relatively low high temperature strength of V limits the maximum use temperature to perhaps 500°C. Nb and Ta alloys

Table 8. **Composition of Select Refractory Metal Alloys**

Alloy designation	Composition, wt%
Nb-1Zr	Nb-1Zr
WC-103	Nb-10Hf-1Ti
FS-85	Nb-27Ta-10W-1Zr
PWC-11	Nb-1Zr-0.1C
Ta-10W	Ta-10W
Ta-111	Ta-8W-2Hf
Ta-222	Ta-10W-2.5Hf-0.01C
Astar 811C	Ta-8W-1Re-1Hf-0.025C
Mo-TZM	Mo-0.5Ti-0.1Zr-0.03C
Mo-42Re	Mo-42Re
W-3Re	W-3Re
W-5Re	W-5Re
W-25Re	W-25Re
W-4Re-0.3Hf-0.025C	W-4Re-0.3Re-0.025C
W-24Re-0.3Hf-0.025	W-24Re-0.3Hf-0.025
W-1ThO_2	W-1ThO_2

exhibit much higher temperature capabilities, but require extensive alloying to achieve useful strength levels.

Many of the refractory metal alloys utilize high levels of the interstitial elements carbon and nitrogen, to form dispersions of carbide, nitrides and carbonitrides (56). This dispersion hardening is very effective to high temperatures and is used in W, Nb, and Nb alloys. The carbide formers typically added to these alloys are Hf and Zr. The alloys of Nb, Ta and Mo are widely available in a variety of mill forms. Due to their high melting points, these alloys are usually processed by powder metallurgy techniques or arc melting in vacuum/inert environments. Although the fabricability of Mo is significantly less than Nb and Ta, wrought processing techniques have been developed to produce all of these alloys in sheets, billet, tubes, bars and special shapes. The processing of W has been highly developed due to its vital use in lamp and electron tube filaments.

In many high temperature applications in the electrical and electronics industry and for many space applications, refractory metals are the best materials. In these applications, the metals are protected by the vacuum or inert gas from oxidation. However, for most other high temperature applications, poor oxidation resistance has limited the use of refractory metals. The oxides of the refractory metals do not exist as thin, adherent and protective scales, like in Ni- and Co-base superalloys. Instead, the oxides of refractory metals are present as rapidly growing, porous oxides at intermediate temperatures and often become volatile at elevated temperatures, and will either spall off of the substrate or vaporize to a gaseous state (57). The surface oxides of these refractory metals volatilize at temperatures significantly below the desired use temperatures, with MoO_3 becoming volatile at about 790°C, WO_3 becoming volatile at about 900°C and Nb_2O_5 becoming volatile at about 1250°C.

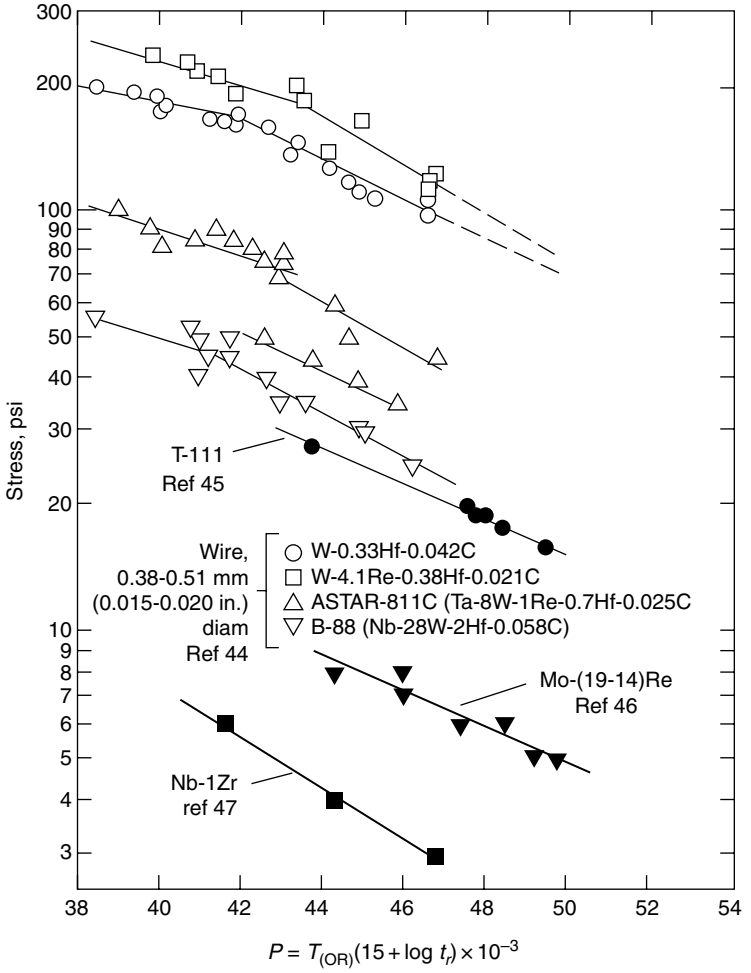

Fig. 26. Larson-Miller plot of stress rupture properties of several refractory metal alloys.

In addition to the rapid, porous scale growth of the refractory metal oxides, the oxide scales are also permit ease gas diffusion of oxygen to the metal surface. This gas transport to the metal surface can, in some cases, be even more damaging than the metal-loss occurring at the surface. The resulting diffusion of oxygen into the base metal results in reductions in ductility and toughness.

In order to use the refractory metal alloys in oxygen containing environments at high temperatures, the alloys must be coated. The most common and most successful coatings applied to the refractory metals are disilicides of the base metal. The coatings are typically 2–5 mm thick and are usually applied by pack cementation techniques, but can also be applied by plasma spraying. Aluminide coatings have also been successfully used on refractory metal components. In general, these types of coatings have been used for applications up to about 1500°C.

Another problem that must be considered when using the refractory metals is joining. As noted previously, thermo-mechanical processing is often needed to obtain ductility in the refractory metals. However, the fusion welding, which requires an inert environment, will often result in recrystallization in the heat affected zone, which results in a significant lose of strength and ductility. Brazing of refractory metals can prevent the occurrence of recrystallization, since it is a lower temperature process, but braze joints do not exhibit the same temperature capabilities as the base metal. Some of these difficulties can be overcome with more exotic welding techniques, such as electron beam welding.

8.3. Ordered Intermetallic Alloys. Alloys based on ordered intermetallic compounds have been the subject of intense investigation during the 1960s and the 1980s (58). In theory, intermetallic compounds offer many attractive properties for high temperature applications. Due to the long range order that is present in intermetallic compounds, most diffusion controlled processes, such as diffusion, creep, recrystallization and oxidation, are slowed. The presence of the long range order results in a significant increase in the activation energy for these thermally activated processes. Many attempts have been made to develop an alloy with useful engineering properties based on the aluminides of Ti, Fe and Ni and the silicides of Ti, Mo and Nb. These aluminide and silicide systems have been selected since these alloys have significant quantities of the lighter Al and Si, which results in an alloy with decreased density. In addition, the high levels of Al and Si offers the potential for excellent oxidation resistance from the formation of either Al_2O_3 or SiO_2 surface scales. There has been some recent work on Nb-based alloys and intermetallics and Mo-Si-B intermetallic alloys for elevated temperature applications (59,60). Significant increases in oxidation resistance has been achieved in the Nb-based and Mo-based alloys systems. However, the ductility and toughness of these alloys is still limited and may preclude their use for structural components.

BIBLIOGRAPHY

"High Temperature Alloys" in *ECT* 2nd ed., Vol. 11, pp. 6–34, by F. J. Clauss, Lockheed Missiles & Space Co.; in *ECT* 3rd ed., Vol. 12, pp. 417–458, by N. S. Stoloff and S. R. Shatynski, Rensselaer Polytechnic Institute; in *ECT* 4th ed., Vol. 13, pp. 237–289, by N. S. Stoloff, Rensselaer Polytechnic Institute; "High Temperature Alloys" in *ECT* (online), posting date: December 4, 2000, by N. S. Stoloff, Rensselaer Polytechnic Institute.

CITED REFERENCES

1. J. R. Davis, "Mechanical Properties at Elevated Temperatures", in J. R. Davis, ed., *ASM Specialty Handbook–Heat Resistant Materials*, ASM, Materials Park, OH, 1997, p. 13.
2. J. R. Davis, "Design for Elevated Temperature Applications", in Ref. 1, p. 518.
3. G. E. Dieter, "Creep and Stress Rupture", in *Mechanical Metallurgy*, 3rd ed., McGraw-Hill, New York, 1986, p. 432.
4. D. A. Woodford, *Met Trans A* **29A**, 2645 (1998).

5. B. J. Piearcey and C. K. Bullough, "An On-Line Materials Database for the Design of Gas Turbine Components", Presented at the International Gas Turbine & Aeroengine Congress & Exhibition, Orlando, Fa., June 2–5, 1997.
6. D. A. Woodford, *Mat. Sci. Eng.* **15**, 169 (1974).
7. C. K. Bullough, "Experience in Applying the New UK Procedure for Creep Rupture Data Assessment to Gas Turbine Materials", Presented at the International Gas Turbine & Aeroengine Congress & Exhibition, Orlando, Fa., June 2–5, 1997.
8. J. B. Conway, *Numerical Methods for Creep and Rupture Analysis*, Gordon and Breach, New York, 1967.
9. R. M. Goldhoff, *Journal of Testing* **1** and **2** (1979).
10. F. R. Larson and J. Miller, *Trans. ASME* **74**, 765 (1952).
11. "Standard Recommended Practice for Conducting Creep, Creep-Rupture and Stress-Rupture Tests of Metallic Materials", E 139, *Annual Book of ASTM Standards, Vol. 03.01*, ASTM, Philadelphia, Pa., 1984, pp. 283–297.
12. "Creep and Stress Relaxation Testing", *ASM Handbook, Tenth Edition*, Vol. 8, 2000, pp. 359–411.
13. J. R. Davis, "Assessment and Use of Creep Rupture Data", in Ref. 1, p. 441.
14. *ASME Boiler and Pressure Vessel Code*, Section1, ASM E.
15. R. M. Goldhof, "Appendix 3: Time-Temperature Parameters", *ASM Metals Handbook*, Vol 3, 9th ed., ASM International, Metals Park, Ohio, 1980, p. 237.
16. R. M. Goldhof, "The Evaluation of Elevated Temperature Creep and Rupture Strength Data: An Historical Perspective", in *Characterization of Materials for Service at Elevated Temperatures*, ASME, New York, 1968, p. 247.
17. S. S. Manson, "Time-Temperature Parameters – A Re-evaluation and Some New Approaches", in *Time-Temperature Parameters for Creep Rupture Analysis*, ASM, Metal Park, Ohio, 1969.
18. G. E. Dieter, "Mechanical Metallurgy – Third Edition", *Fatigue of Metals*, McGraw Hill, Inc., New York, 1986, p. 375.
19. S. T. Rolfe and J. M. Barsom, *Fracture and Fatigue Control in Structures: Applications of Fracture Mechanics*, Prentice-Hall, Inc., Englewoods, N. J., 1977, p. 208.
20. S. T. Rolfe and J. M. Barsom, *Fracture and Fatigue Control in Structures: Applications of Fracture Mechanics*, Prentice-Hall, Inc., Englewoods, N. J., 1977, p. 232.
21. R. W. Hertzberg, *Deformation and Fracture Mechanics of Engineering Materials*, John Wiley & Sons, Inc., New York, 1976, p. 415.
22. Ref. 21.
23. "Mechanical Testing", *Metals Handbook*, 10th ed., Vol. 8, Fatigue Testing, ASM International, Materials Park, Ohio, 2000, p. 679.
24. "Fatigue and Fracture", *Metals Handbook*, 10th ed., Vol. 19, ASM International, Materials Park, OH, (1996).
25. R. F. Decker, *Proc. Steel Strength. Mech. Symp.*, Climax Molybdenum Company, Greenwich, Conn., Zurich, May 5–6, 1964, Vol 1, p. 147.
26. R. L. Fleischer, *Acta Met.* **11**, 203 (1963).
27. O. Noguchi, Y. Oya, and T. Suzuki, *Met Trans A* **12A**, 1647 (1981).
28. R. M. N. Pelloux and N. J. Grant, *Trans. Met. Soc. AIME* **218**, 232 (1960).
29. N. F. Mott and F. R. N. Nabarro, *Rep. Conf. Strength. Sol. Phys. Soc.* 1–9 (1948).
30. E. Orowan, *Symp. On Internal Stresses in Metals*, Institute of Metals, London, 1948, p. 451.
31. M. W. Cockell and K. A. G. Boyce, *Met Powder Rev.* **40**(3), 139 (1985).
32. F. S. Pettit, *Trans. TMS-AIME* **239**, 1296 (1967).
33. E. Fitzer and J. Schlichting in R. A. Rapp ed., *High Temperature Corrosion*, NACE, Houston, Texas, 1983, p. 604.

34. J. R. Davis, "Design for Oxidation Resistance", in Ref. 1, p. 534.
35. J. R. Davis, "Corrosion at Elevated Temperatures", in Ref. 1, p. 31.
36. R. L. Jones, "Hot Corrosion in Gas Turbines", in *Corrosion in Fossil Fuel Systems*, The Electrochemical Society, Princeton, N. J., 1983, p. 341.
37. J. Stringer, in Ref. , p. 389.
38. G. W. Goward and D. H. Boone, *Oxid Met.* **3**, 475 (1971).
39. J. R. Davis, "Refractory Metals and Alloys", in Ref. 1, p. 361.
40. J. R. Davis, *Nickel, Cobalt and Their Alloys, ASM Specialty Handbook*, ASM International, Materials Park, Ohio, 2000.
41. J. R. Davis, *Heat-Resistant Materials, ASM Specialty Handbook*, ASM International, Materials Park, Ohio, 1997.
42. C. T. Sims, N. S. Stoloff, and W. C. Hagel, eds., *Superalloys II*, John Wiley & Sons Inc., New York, 1987.
43. S. J. Rosenberg, *Nickel and It's Alloys, National Bureau of Standards Monograph 106*, U.S. Department of Commerce, May 1968.
44. W. Betteridge, *Nickel and Its Alloys*, Ellis Horwood Ltd., 1984.
45. G. Vroman, *American Metal Market*, 10A-11A (Oct. 1998).
46. D. Furrer and H. Fecht, *JOM*, 14–18 (Jan. 1999).
47. R. L. Fleischer, *The Strengthening of Metals*, Reinhold, New York, 1964, p. 93.
48. N. S. Stoloff, "Fundamentals of Strengthening", in C. T. Sims, N. S. Stoloff and W. C. Hagel, eds., "*Superalloys II*", John Wiley & Sons, Inc., New York, 1987, p. 61.
49. E. E. Brown and D. R. Muzyka, "Nickel-Iron Alloys", in Ref. 48, p. 165.
50. R. F. Decker, "Strengthening Mechanisms in Nickel-base Superalloys", *Presented at Steel Strengthening Mechanisms Symposium*, Zurich, Switzerland, May 5 and 6, 1969.
51. "High Temperature, High Strength, Nickel Base Alloys", International Nickel Company, Saddle Brook, N. J., 1984.
52. J. R. Davis, "Uses of Cobalt", in *Nickel, Cobalt and Their Alloys, ASM Specialty Handbook*, ASM International, Materials Park, Ohio, 2000, p. 349
53. J. R. Davis, "Corrosion Behavior of Cobalt Alloys", in *Nickel, Cobalt and Their Alloys, ASM Specialty Handbook*, ASM International, Materials Park, Ohio, 2000, p. 395.
54. J. R. Davis, "Properties of Cobalt Alloys", in Ref. 53, p. 373.
55. A. Asphahani, *Corrosion* **13**, 658 (1987).
56. J. Wadsworth, J. Wittenauer, and T. G. Nieh, "Strengthening and Toughening of Refractory Metal Alloys", in N. S. Stoloff, D. J. Duquette, and A. F. Giamei, eds., *Critical Issues in the Development of High Temperature Structural Materials*, TMS-AIME, Warrendale, Pa, 1993, p. 189.
57. R. W. Buckman, Jr. and R. C. Goodspeed, *Refractory Metal Alloys*, Plenum Press, New York, 1968.
58. J. R. Davis, "Structural Intermetallics", in Ref. 1, p. 389.
59. K. J. Leonard, J. C. Mishurda, and V. K. Vasudevan, *Mat. Sci. and Eng. A.* **A329–331**, 282 (2002).
60. K. Ihara, K. Ito, K. Tanaka, and M. Yamaguchi, *Mat. Sci. and Eng. A.* **A329–331**, 222 (2002).

G. E. FUCHS
Materials Science & Engineering